Current Trends in MASS Spectrometry

SUPPLEMENT TO
October 2017
LCGC North America | *LCGC Europe* | *Spectroscopy*

GC–MS Analysis of Antimicrobial Agents in Vegetable Oil

Unraveling the Heterogeneity of Glycoproteins with Mass Spectrometry

Nontargeted LC–MS/MS for Toxic Compound Identification

UBM

UNBELIEVABLY POWERFUL
REMARKABLY SMALL

IT'S TIME TO SET A PINT-SIZED POWERHOUSE LOOSE IN YOUR LAB.

Meet Agilent's new, revolutionary Ultivo Triple Quadrupole LC/MS. It's packed full of the same power and accuracy you'll find in the big guys but at a fraction of the size. It's on a transformative mission to reshape expectations, reinvent capabilities, and redefine what's possible when small meets powerful.

You don't need to change the game, just how you play it.
Discover remarkable at agilent.com/chem/ultivo

Agilent Technologies

SHIMADZU
Excellence in Science

Seamless Integration of Sample Preparation to LC-MS/MS Analysis

Simplify workflows and improve lab efficiency with Shimadzu's industry-first automated sample prep module

Shimadzu's **CLAM-2000** Clinical Laboratory Automation Module is a fully automated sample prep module for LC-MS/MS that integrates common clinical sample prep workflows, such as protein precipitation and chemical derivatization, to the mass spec. By requiring no intervention from sample loading to results, it improves data reproducibility and accuracy, provides uniform pretreatment times between samples, and minimizes operator error.

Learn more about Shimadzu's CLAM-2000. Call (800) 477-1227 or visit us online at **www.ssi.shimadzu.com/CLAM**

Order consumables and accessories on-line at http://store.shimadzu.com
Shimadzu Scientific Instruments Inc., 7102 Riverwood Dr., Columbia, MD 21046, USA
For Research Use Only. Not for use in diagnostic procedures.

Key features/benefits include:

- **Offers exceptional data accuracy and reproducibility by performing all processes from pretreatment of samples to analysis automatically.**
- **Increases laboratory efficiency by processing each sample successively in parallel.**
- **Allows any level of user to prepare samples and operate the LCMS like an expert using a simplified user interface.**
- **Provides a flexible platform to suit the specific application's needs.**

LCGC north america solutions for separation scientists | LCGC europe solutions for separation scientists | Spectroscopy®

MANUSCRIPTS: To discuss possible article topics or obtain manuscript preparation guidelines, contact the editorial director at: (732) 346-3020, e-mail: Laura.Bush@ubm.com. Publishers assume no responsibility for safety of artwork, photographs, or manuscripts. Every caution is taken to ensure accuracy, but publishers cannot accept responsibility for the information supplied herein or for any opinion expressed.

SUBSCRIPTIONS: For subscription information: *Spectroscopy,* P.O. Box 6196, Duluth, MN 55806-6196; (888) 527-7008, 7:00 a.m. to 6:00 p.m. CST. Outside the U.S., +1-218-740-6477. Delivery of *Spectroscopy* outside the U.S. is 3–14 days after printing. Single-copy price: U.S., $10.00 + $7.00 postage and handling ($17.00 total); Canada and Mexico, $12.00 + $7.00 postage and handling ($19.00 total); Other international, $15.00 + $7.00 postage and handling ($22.00 total).

CHANGE OF ADDRESS: Send change of address to *Spectroscopy,* P.O. Box 6196, Duluth, MN 55806-6196; provide old mailing label as well as new address; include ZIP or postal code. Allow 4–6 weeks for change. Alternately, go to the following URL for address changes or subscription renewal: http://ubmsubs.ubm.com/?pubid=SPEC

RETURN ALL UNDELIVERABLE CANADIAN ADDRESSES TO: IMEX Global Solutions, P.O. Box 25542, London, ON N6C 6B2, CANADA. PUBLICATIONS MAIL AGREEMENT No.40612608.

REPRINT SERVICES: Reprints of all articles in this issue and past issues are available (500 minimum). Call 877-652-5295 ext. 121 or e-mail bkolb@wrightsmedia.com. Outside US, UK, direct dial: 281-419-5725. Ext. 121

C.A.S.T. DATA AND LIST INFORMATION: Contact Melissa Stillwell, (218) 740-6831; e-mail: Melissa.Stillwell@ubm.com

INTERNATIONAL LICENSING: Maureen Cannon, (440) 891-2742, fax: (440) 891-2650; e-mail: Maureen.Cannon@ubm.com

50% Recycled Paper 10-20% Post Consumer Waste | Alliance for Audited Media | Connectiv

UBM Americas (www.ubmamericas.com) is a leading worldwide media company providing integrated marketing solutions for the Fashion, Life Sciences and Powersports industries. UBM Americas serves business professionals and consumers in these industries with its portfolio of 91 events, 67 publications and directories, 150 electronic publications and Web sites, as well as educational and direct marketing products and services. Market leading brands and a commitment to delivering innovative, quality products and services enables UBM Americas to "Connect Our Customers With Theirs. UBM Americas has approximately 1000 employees and currently operates from multiple offices in North America and Europe.

485F US Highway One South, Suite 210
Iselin, NJ 08830
(732) 596-0276
Fax: (732) 647-1235

Michael J. Tessalone
Vice President/Group Publisher
Michael.Tessalone@ubm.com

Stephanie Shaffer
Publisher
Stephanie.Shaffer@ubm.com

Edward Fantuzzi
Associate Publisher
Edward.Fantuzzi@ubm.com

Brianne Molnar
Sales Manager
Brianne.Molnar@ubm.com

Michael Kushner
Senior Director, Digital Media
Michael.Kushner@ubm.com

Laura Bush
Editorial Director
Laura.Bush@ubm.com

Megan L'Heureux
Managing Editor
Meg.L'Heureux@ubm.com

Stephen A. Brown
Group Technical Editor
Stephen.Brown@ubm.com

Cindy Delonas
Associate Editor
Cindy.Delonas@ubm.com

Kristen Moore
Webcast Operations Manager
Kristen.Moore@ubm.com

Vania Oliveira
Project Manager
Vania.Oliveira@ubm.com

Sabina Advani
Digital Production Manager
Sabina.Advani@ubm.com

Kaylynn Chiarello-Ebner
Managing Editor, Special Projects
Kaylynn.Chiarello.Ebner@ubm.com

Dan Ward
Art Director
dward@hcl.com

Anne Lavigne
Marketing Manager
Anne.Lavigne@ubm.com

Melissa Stillwell
C.A.S.T. Data and List Information
Melissa.Stillwell@ubm.com

Wright's Media
Reprints
bkolb@wrightsmedia.com

Maureen Cannon
Permissions
Maureen.Cannon@ubm.com

Jesse Singer
Production Manager
jsinger@hcl.com

Wendy Bong
Audience Development Manager
Wendy.Bong@ubm.com

Ross Burns
Audience Development Assistant Manager
Ross.Burns@ubm.com

Eliminate ~~gas cylinders~~ today!

Discover a better way with VICI DBS gas generators.

ELIMINATE HIGH PRESSURE GAS CYLINDERS TO:

- ✕ Improve lab safety
- ✕ Reduce lab expenses due to costly gas refills and cylinder rental fees
- ✕ Prevent instrument downtime due to running out of cylinder gas

DISCOVER HOW VICI GAS GENERATORS:

- ✓+ Are the smart safe alternative
- ✓+ Can pay for themselves immediately by saving money on gases
- ✓+ Provide an endless supply of research grade gas
- ✓+ Include a 2 year warranty

VICI DBS™

www.vicidbs.com

Hydrogen Nitrogen Zero Air

800-367-8424 | infousa@vicidbs.com

Current Trends in
MASS
Spectrometry

October 2017

Articles

Departments

Cover image courtesy of venars.original / shutterstock.

Gas Chromatography–Mass Spectrometry Characterization of Vegetable Oil–Derived Potent Antimicrobial Agents

Under a suitable thermal oxidation regime, vegetable oils yield a mixture of volatile and semivolatile organics that exhibit very high antimicrobial activities against a variety of microbial species. Volatile and semivolatile products were characterized with gas chromatography–mass spectrometry (GC–MS) equipped with electron ionization (EI) and chemical ionization (CI) sources. The GC–MS results showed that the antimicrobial mixture comprised short and medium chain organic acids, aldehydes, and ketones, including propanal, butanal, hexanal, octanal, nonanal, propionic acid, hexanoic acid, heptanoic acid, and octanoic acid. Microbial exposure experiments showed that a short exposure period of less than 2 min was effective in killing vegetative bacterial cells with efficiencies as high as 10^9. The present report deals primarily with chemical characterization of the volatile and semivolatile organics with GC–MS.

Racha Seemamahannop, Prakash Wadhawa, Shubhen Kapila, and Abha Malhotra

Rising concerns for resistance of microbial species to specific antibiotics have aroused interest in nonspecific broad-spectrum disinfectants (1). Selected plant species have been noted for possessing antimicrobial activities since prehistoric times, and renewed interest has been generated toward plant-based antimicrobial agents. Considerable attention is being paid to plant-derived oils and extracts as broad-spectrum disinfectants. Essential oils obtained through hydrodistillation of basil plants (*Ocimum basilicum*) were found to contain terpene alcohols (linalool) and exhibited strong antifungal activity (2). Antibacterial and antifungal activity of eucalyptus wood (*Eucalytus glubulus*) extracts have also been reported and noted the presence of gallic acid, ellagic acid, and citric acid (3).

Similarly, the generation and use of oil-derived disinfectants was described in ancient times—for example, the ancient Indian text "Vedas" describes purification rituals that involve offering clarified butter (ghee) to the fire god Agni. The text states that the offering does not destroy the components, but transforms constituents into minuscule constituents that can purify the environment by the elimination of harmful organisms (4,5). However, the chemicals produced or the chemical transformation of oils during the ritual has not been described in open literature. Chemical transformation of vegetable oils during storage at ambient temperatures and during food preparation has been studied and reviewed extensively (6–11). The emphasis of such studies have been on the production of off-flavor compounds, such as aldehydes, and the generation of trans fatty acids. Although the production of aldehydes and ketones from the autooxidation of polyunsaturated fats and oils has been known for some time, the antimicrobial activity of such oxidation products derived from biogenic oils has not been reported in the literature.

Oil-based obscurant generation involves a process that is somewhat similar to the ancient Vedic rituals and involves volatilization of oils at high temperatures. Under ambient temperatures vapors condense to form aerosols—droplets with diameters ranging from 0.5 to 2 μm. Such droplets when present

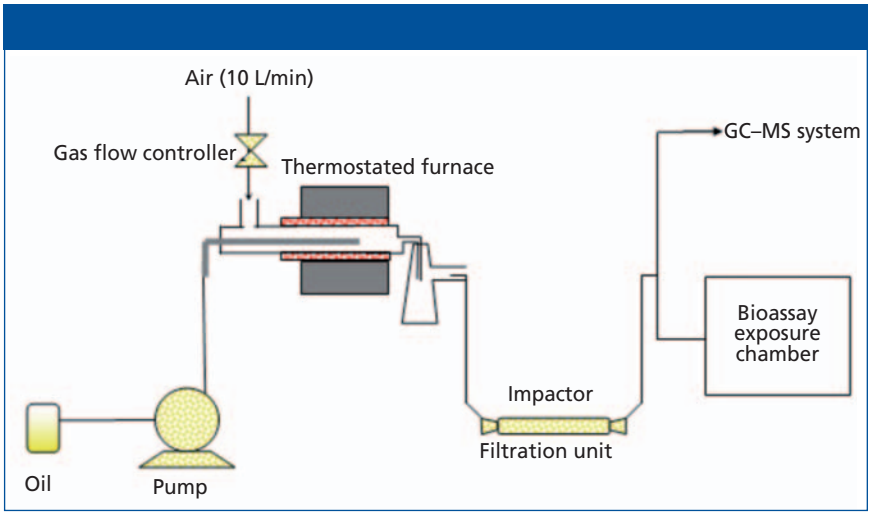

Figure 1: A schematic of the bench-scale vapor generation, exposure, and gas sampling setup.

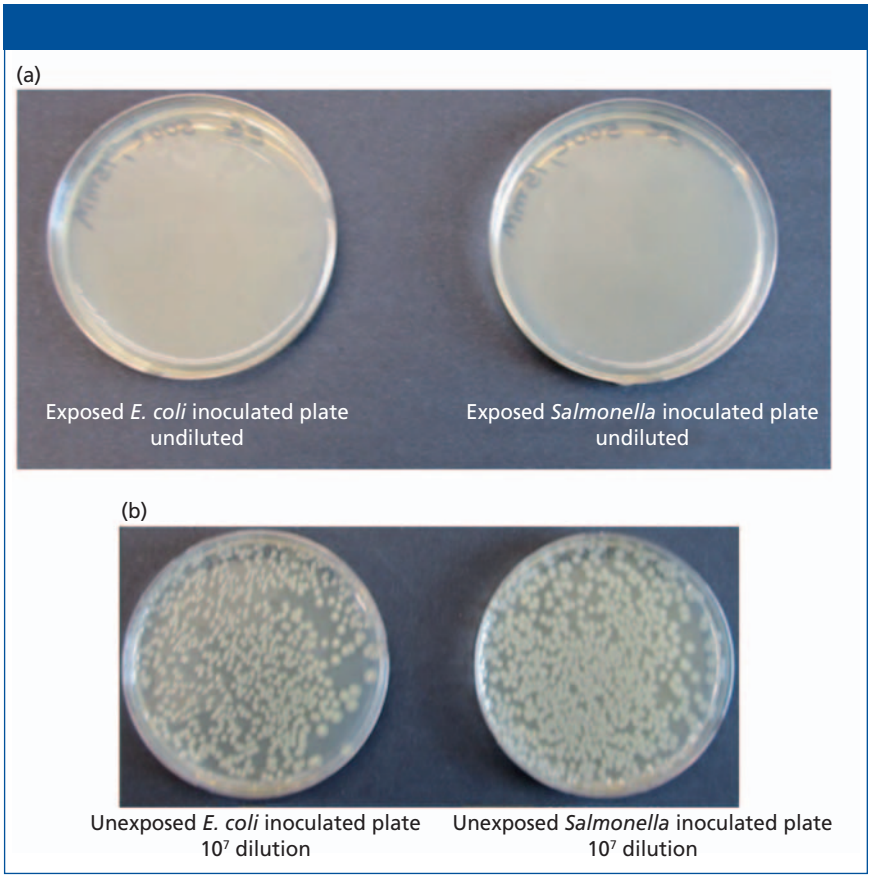

Figure 2: Comparison of bacterial cultures (a) exposed to soybean oil–derived disinfectant vapors and (b) diluted unexposed cultures.

in high concentrations are very effective in scattering visible and near-infrared (NIR) radiation, forming a "fog" or obscurant medium (12,13). During laboratory simulation experiments to assess the mutagenicity of the aerosols it was discovered that when aerosols or vapors are generated under suitable oxidation regimes, an extremely potent antimicrobial mixture is formed. Experiments carried out to date have shown that the process permits generation of a highly effective wide-spectrum microbicidal–sporicidal chemical vapor from nontoxic oils. The process involves controlled pyrolytic oxidation of a relatively innocuous substance such as hydrocarbon based mineral oils, or preferably natural esters (vegetable oils or their monoesters), leading to the generation of a mixture of antimicrobial agents including volatile organic acids, aldehydes and ketones. The mixture has exhibited exceptional antimicrobial activity.

A study was initiated to quantify disinfectant efficiency of the oil-derived vapors against a variety of pathogenic microbial species including Gram-positive and -negative bacteria, bacterial spores, fungal spores, and viruses. Tandem experiments were carried out to characterize major volatile and semivolatile constituents of the oil-derived disinfectant vapors. Characterization was carried out with a tandem gas chromatography–mass spectrometry (GC–MS) system. The results showed that under suitable conditions thermal oxidation of vegetable oils resulted in the formation of short and medium chain acids, aldehydes, and ketones that act synergistically to yield a very potent microbial disinfectant.

Experimental

Volatilization and Transformation Oils

The bench-top setup for volatilization of oils consisted of a 40 cm × 1.25 cm (o.d.) stainless steel tube. The tube was placed in an electrically heated tubular furnace. The temperature of the furnace was controlled with a feedback type temperature control unit; temperature of the reactor was monitored and controlled with a feedback circuit. Oils were introduced into the stainless steel tube with a reciprocating piston pump at flow rates of 0.25 or 0.5 mL/min. Gas (air or argon) flow through the tube was controlled with a mass flow controller and varied between 2 and 10 L/min. The volatilization temperature was varied from 350 °C to 600 °C (±5 °C). Oil and gas were introduced in to the reactor tube through a concentric tube arrangement. A simple schematic of the setup is shown in Figure 1. The split stream setup of the generation system allowed simultaneous execution of microbial toxicity assay and chemical characterization of volatile organics.

Soybean oil used during the experiment was purchased locally and methyl soyate was purchased from AG Environmental Products L.L.C. Other vegetable oils used during the experiments included linseed oil, olive oil, and corn oil, which were all obtained locally. Fog oil was obtained from

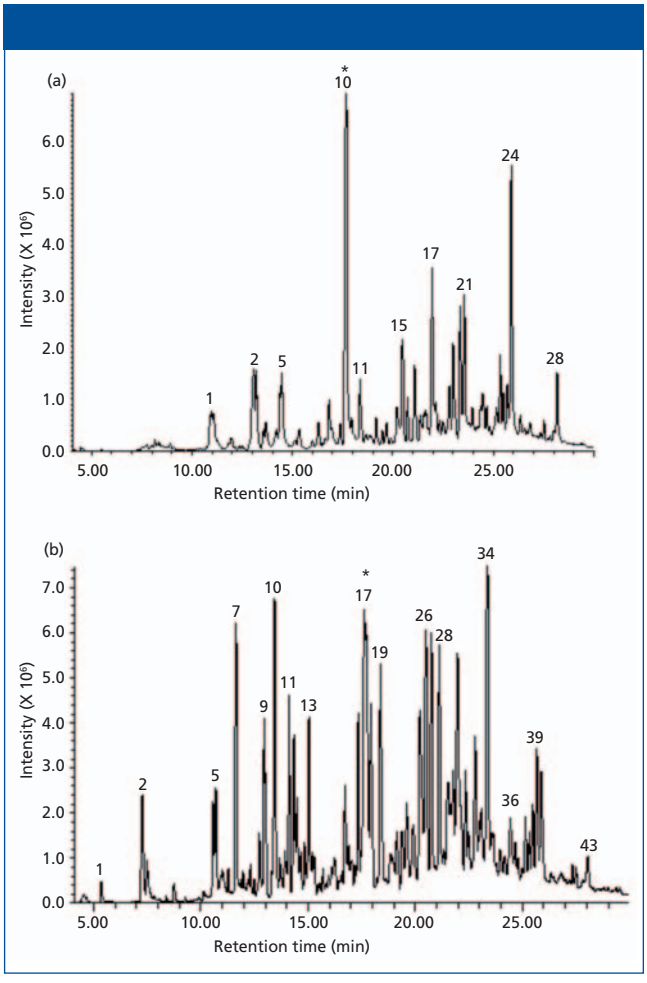

Figure 3: TICs of volatile organics in vapors streams from soybean oil volatilized at (a) 400 °C and (b) 550 °C.

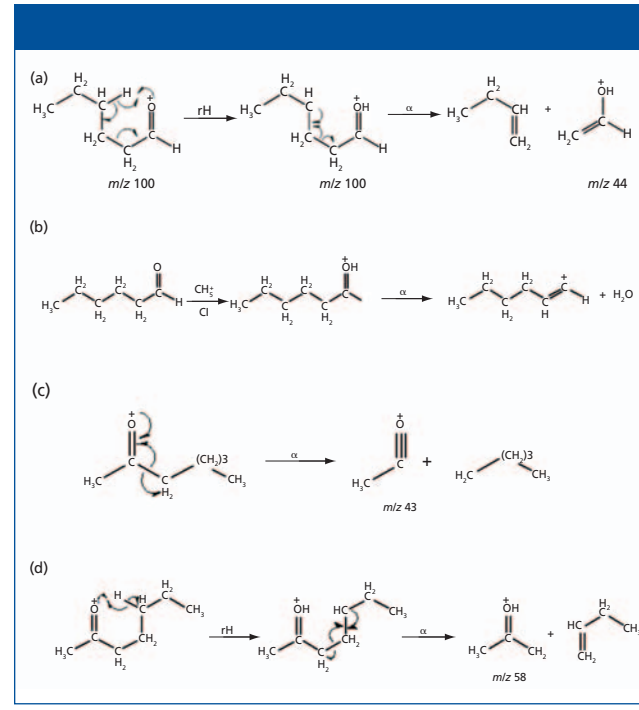

Figure 4: Fragmentation of (a) hexanal molecular ion in the EI spectrum, (b) hexanal pseudomolecular ion in the CI spectrum, (c) 2-heptanone molecular ion in the EI spectrum, and (d) 2-heptanone following γH rearrangement in EI spectrum.

the U.S. Army Chemical School. Fog oil is a middle distillate of petroleum similar to the commercially available mineral oil. It is used for the generation of smoke (osbcurant) screens through vaporization and condensation processes.

Microbial Tests

The bacterial species were precultured in 5 mL of nutrient broth without shaking at room temperature for 12 h. The absorbance of the preculture was observed at 560 nm. The preculture was used when the absorbance readings reached between 0.6 and 0.8. A 150-µL aliquot of the preculture was diluted with 850 µL of nutrient broth. Two 10-µL drops of the diluted preculture were added to a nutrient agar plate. For the toxicity assay, the nutrient agar plates were exposed to vapors for 2, 5, or 10 min in the exposure chamber. The plate was incubated at 37 °C for 24 h and examined for the presence of bacterial colonies.

Chemical Characterization of Volatiles and Semivolatiles with GC–MS

The chemical characterization of vapors was carried out with a GC–MS system consisting of a Varian 3800 gas chromatograph interfaced to a Varian 920 mass spectrometer. Characterization of volatile components was facilitated with a cryotrap and a six-port sampling valve (model C6W, Valco Instruments). An aliquot of the vapor stream was transferred from the gas sampling bulb into the GC column with the six-port valve. The valve was mounted inside the column oven and maintained at the oven temperature. A fused-silica tube with a volume of 50 µL served as the sampling loop. During the sampling mode, the gas sample was pulled through the loop with a low-volume vacuum pump at a flow rate of 30 mL/min. At the end of the sampling period, the valve was switched to transfer the sample into the GC column.

GC Parameters

The following GC parameters were used:

Column: 60 m × 0.25 mm (i.d.) fused-silica capillary with a 95% methyl, 5% phenyl polysiloxane stationary phase
Carrier: Helium, ultrahigh purity grade, volume flow rate 1 mL/min
Linear velocity: 28 cm/s
Injection: On-line loop, with a loop volume of 50 µL
Cryogen: CO_2
Cryotrap cycle: Cryogen, switched on 1.50 min before injection, switched off 2.50 min after injection
Oven temperature: -10 °C initial, 3-min hold, then 8 °C/min to a final temperature of 200 °C, hold 4 min

MS Parameters

The MS system comprised a triple-quadrupole analyzer with an electron ionization (EI) and chemical ionization (CI) source. The ion source could be operated in the EI or CI modes. In the EI mode, the electron energy was set at 60 eV.

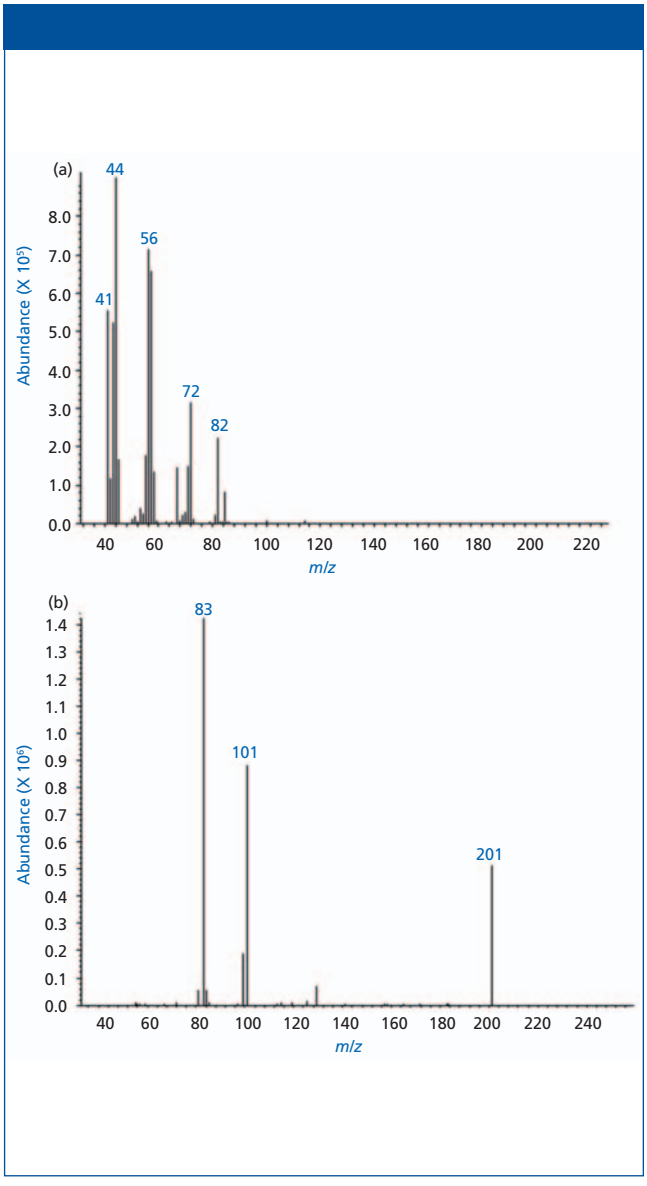

Figure 5: Mass spectra of a predominant peak in the TIC of soybean oil volatilized at 400 °C: (a) EI, (b) CI.

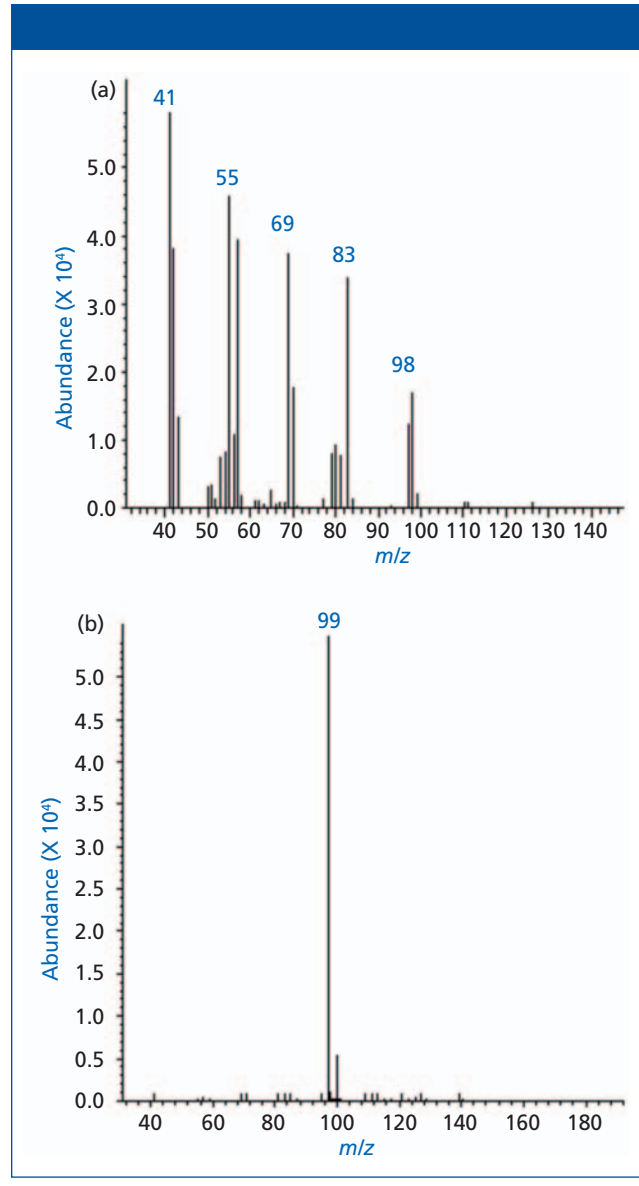

Figure 6: Mass spectra of another strong peak in the TIC of soybean oil volatilized at 550 °C: (a) EI, (b) CI.

Methane was used as the reagent gas in the CI mode. The mass spectrometer was operated in the scan mode over a range of 40–450 amu. The scan speed was set at 0.5 s.

Results and Discussion

Microbial Exposure Results

The efficacy of the oil-derived vapor in controlling vegetative bacterial cell growth was assessed by examining agar plates inoculated with several bacterial strains including *Escherichia coli* and *Salmonella typhimurium*. Undiluted bacterial cultures were applied to nutrient agar plates and exposed to the oil-derived vapors. The agar plates inoculated with diluted bacterial culture were used as the controls and the dilution factor was ten million or one hundred million fold, that is, 1×10^7 or 1×10^8. All exposures were carried out at ambient temperature for time periods of 2–15 min for the vegetative bacterial cultures and up to 1 h for the bacterial and fungal spores. Exposed and control plates were incubated at 37 °C for 24 h. The plates were examined for colonies on the exposed and control plates. A quantitative measure of disinfectant efficiency was made on the basis of the number of colonies on the exposed plates with undiluted cultures and unexposed plates with diluted bacterial cultures.

> Disinfection efficiency = [number of colonies on the exposed plate × dilution / number of colonies on the control (unexposed) plates × dilution/]

For example, the number of colonies on the unexposed plates inoculated with diluted (1×10^8) *Salmonella typhimurium* culture was found to be 66. There were no colonies observed on the exposed plate with undiluted culture when exposed to vapors generated through volatilization of soybean oil at 550 °C. The disinfection efficiency for *Salmonella typhimurium* after exposure to soybean oil-derived vapors was estimated to be 66×10^8

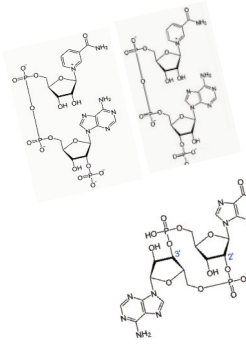

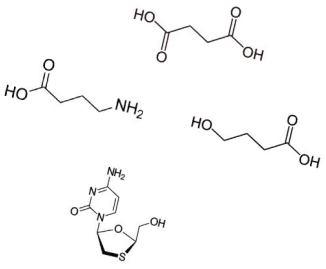

iHILIC® -Fusion

New HILIC Applications for HPLC and UHPLC

"A Very Versatile Chemistry"

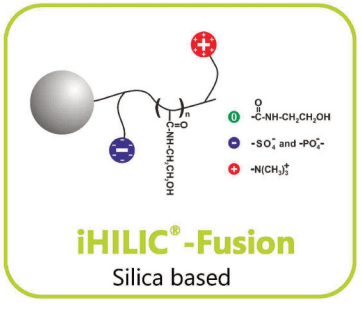

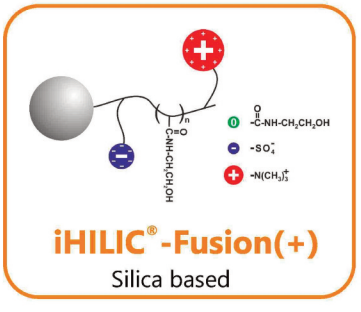

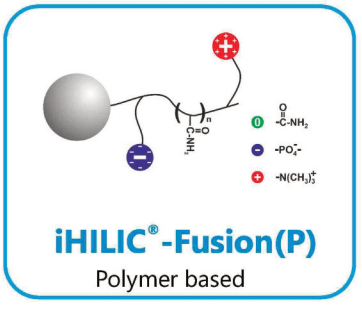

Nucleotides

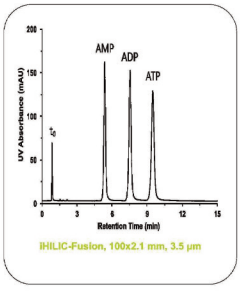

iHILIC-Fusion, 100x2.1 mm, 3.5 µm

Phospholipids

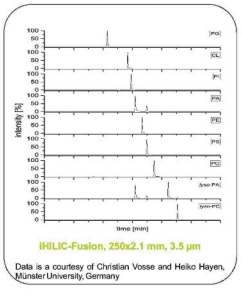

iHILIC-Fusion, 250x2.1 mm, 3.5 µm

Data is a courtesy of Christian Vosse and Heiko Hayen, Münster University, Germany

Amino Acids

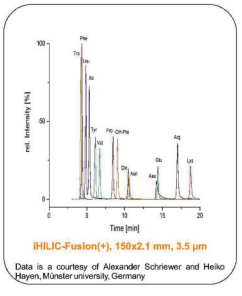

iHILIC-Fusion(+), 150x2.1 mm, 3.5 µm

Data is a courtesy of Alexander Schriewer and Heiko Hayen, Münster university, Germany

Cell Metabolites

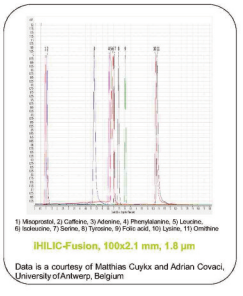

iHILIC-Fusion, 100x2.1 mm, 1.8 µm

Data is a courtesy of Matthias Cuykx and Adrian Covaci, University of Antwerp, Belgium

Artificial Sweeteners

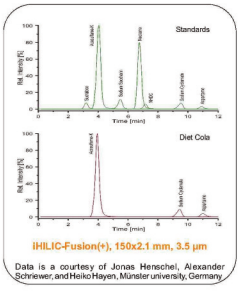

iHILIC-Fusion(+), 150x2.1 mm, 3.5 µm

Data is a courtesy of Jonas Henschel, Alexander Schriewer, and Heiko Hayen, Münster university, Germany

iHILIC Publications

iHILIC-Fusion:
- J. Chromatogr. A, 1478 (2017) 168-178 - Metabolomics
- ChemBioChem, 18 (2017) - UDP-sugar
- LCGC Europe, (2016) September, 537-538 - Metabolomics

iHILIC-Fusion(+):
- LCGC Europe, (2016) July, 401 - Food and Beverage

iHILIC-Fusion(P):
- Cell Reports, 17 (2016) 837–848 - Metabolomics
- Anal. Chem., 89 (2017) 1624−1631 - Metabolomics
- J. Liq. Chromatg. Rel. Technol., (2017) - dithiocarbamate fungicides
- Nature Communications, 8 (2017) - Metabolomics

Features

- Charge modulated hydroxyethyl amide/amide HILIC columns
- Complementary selectivities for polar/hydrophilic analytes
- Excellent durability and ultra-low bleeding for LC-MS
- Perfect columns for ”Omics” studies
- iHILIC®-Fusion and iHILIC®-Fusion(+): pH 2-8; 1.8, 3.5, and 5 µm
- iHILIC®-Fusion(P): pH 1-10; 5 µm

Columns available with 1.8μm, 3.5μm, or 5μm particles and SPE formats

www.nestgrp.com/iHILIC.shtml

New! Semi-Reusable SPE Formats

BioPureSPN™ Color Coded ~ Reusable Spin Columns

VOLUME EFFECTS ON SPE

Desorption Increases From Excessive Sample & Wash Volumes

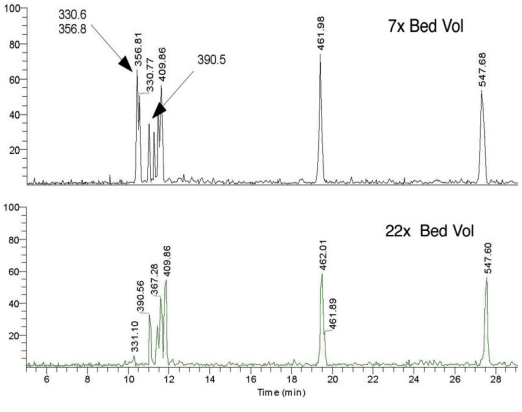

Column: TARGA® C18, 300µm x 30mm Trap
Sample Solvent: 0.1% FA water (volumes as shown). Trap Column in 0.1% FA water
Gradient: 98% water, 0.1% FA, 2% ACN to ACN, 0.1% FA

A Chemistry For Every Compound

Affinity - Empty - ERLIC - HILIC - IEX - RPC - SEC

Product Formats	Sample Capacity	Packed Volume	Void Volume	Elution Volume
UltraMicroSpin™ Column	**3-30 µg**	**30 µL**	**12 µL**	**2-25 µL**
MicroSpin™ Column	**5-60 µg**	**60 µL**	**25 µL**	**5-50 µL**
MACROspin™ Column	**30-300 µg**	**190 µL**	**90 µL**	**25-180 µL**
96-Well MicroSpin™ Plate	**3-30 µg**	**60 µL**	**25 µL**	**5-50 µL**
96-Well MACROspin™ Plate	**30-300 µg**	**190 µL**	**90 µL**	**25-180 µL**
Empty -Reactors™ /w caps			**200 µL**	
Page*Eraser™ Filters		**0.1µL**	**5-200 µL**	
HisSep™ Histidine Removal	**200-500 µg**			

New Products

BioPureSPN™ PROTO™ C18	**3-300 µg**	**20-200 µL**	**10-100 µL**	**5-200 µL**
BioPureSPN™ PROTO™ C4	**3-300 µg**	**20-200 µL**	**10-100 µL**	**5-200 µL**
BioPureSPE™ TARGA® C18	**3-300 µg**	**20-200 µL**	**10-100 µL**	**5-200 µL**
iSPE® Fusion™ HILIC	**0.4 - 1 g**	**50µL-1mL**	**50-500 µL**	**50µL-1mL**

The Nest Group, Inc.

Not Just Columns ... Answers!

45 Valley Road, Southborough, MA 01772 USA
E-mail: sales@nestgrp.biz
For more Info: www.nestgrp.com

or 6.6 × 10^9 fold, or better than nine logs. Similar results were obtained with *Escherichia coli*, unexposed plates with 1×10^8 diluted culture showed an average count of 82 colonies. Whereas not even a single colony was observed on plates exposed to vapors generated from soybean oil, the disinfectant efficiency in this case was calculated to be 82×10^8 or 8.2×10^9, more than nine logs.

Similar results were obtained with other bacterial species, including *Mycobacterium smegmatis*, *Mycobacterium phlei, Salmonella typhimurium, Klebsiella pneumonia, Escherichia coli, Pseudomonas aeruginosa, Enterobacter cloacae, Shigella sonnei, Serratia marcescens, Bacillus subtilis, Bacillus stearothermophilus, Staphylococcus aureus, Staphylococcus epedermis,* and *Streptococcus mutans*. The antimicrobial strength of the vapors was found to depend on the starting oil, volatilization temperature, and gas present during volatilization. Microbial exposure experiments showed that antimicrobial activity depends on the chemical composition of volatile and semivolatiles present in the vapor stream.

Chemical Characterization of Disinfectant Vapors

GC Separation of Volatile Components

Volatile and semivolatile constituents of disinfectant vapors were separated with GC. Separations were carried out with the 60-m fused-silica capillary with a relatively nonpolar stationary phase. To facilitate separation of volatile components, the initial temperature of the GC column oven was set at -10 °C. This initial temperature was selected by monitoring the separation of model analytes such as acetaldehyde, acetone, isopropanol, butanal, butanone, and hexanal. The subambient initial column temperatures minimized the band broadening of volatile analytes and yielded narrower peaks, resulting in superior resolution.

Qualitative and Quantitative Determination of Volatile Components

The qualitative determination of volatile components was carried out using MS with the ion source in EI mode. CI was used for positive confirmation of labile analytes that do not yield molecular ion at satisfactory abundance in the EI mode. The identity of some of the analytes was confirmed through collision induced dissociation (CID) of a pseudomolecular ion obtained with CI. Quantification of all compounds detected in the vapor stream was carried out with the internal standard method. Ion intensities for standard analytes were obtained at four different concentrations over the 1–100 µg/L range. Deuterated benzene (C_6D_6) was used as the internal standard.

Total ion chromatograms (TICs) of "particulate free" gas stream with volatile and semivolatile organics formed during volatilization of soybean oil at 400 °C and

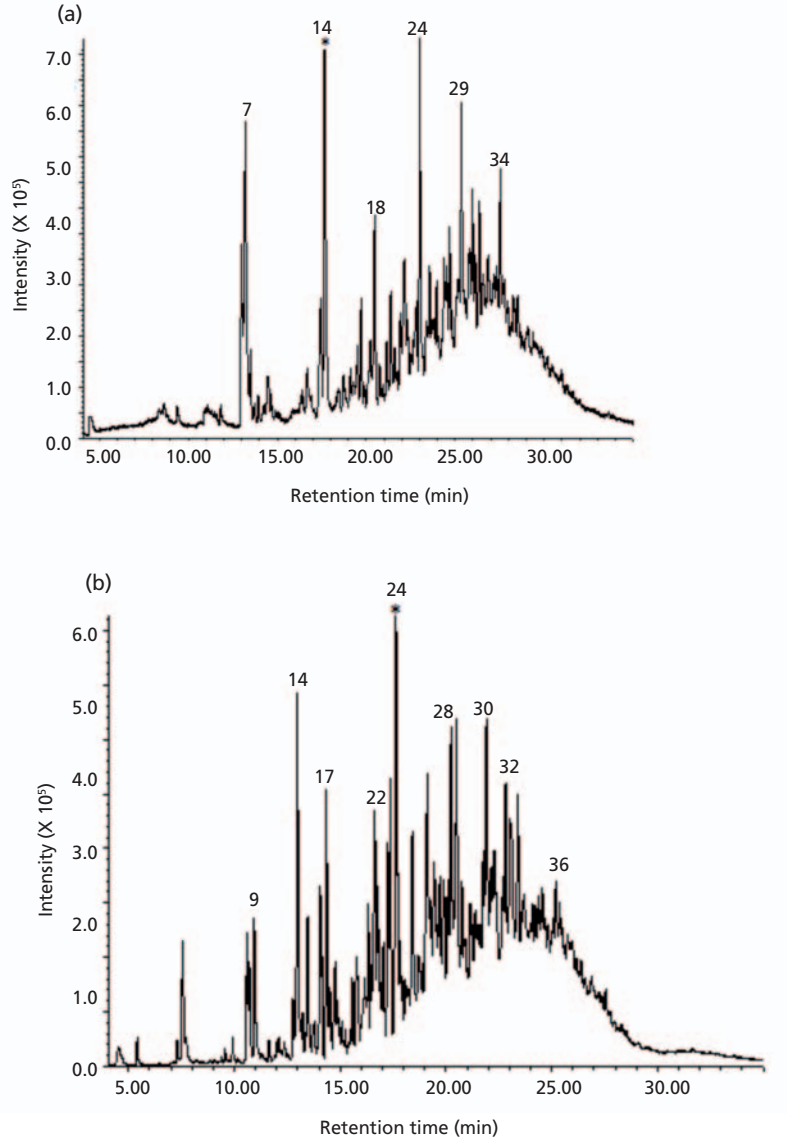

Figure 7: TICs of volatile organics in vapor streams from fog oil volatilized at (a) 400 °C and (b) 550 °C.

Table I: Antimicrobial activities fog oil and soybean oil streams volatilized at different temperatures

Exposure Time	Fog Oil				Soybean Oil			
	400 °C	450 °C	500 °C	550 °C	400 °C	450 °C	500 °C	550 °C
5 min	<log 3	<log 3	<log 3	<log 3	~log 3	~log 6	~log 7	>log 8
10 min	<log 3	<log 3	<log 3	~log 3	~log 3	~log 6	~log 7	>log 8
15 min	<log 3	<log 3	<log 3	~log 3	~log 3	~log 6	~log 7	>log 8
20 min	<log 3	<log 3	~log 3	~log 4	~log 3	~log 6	~log 7	>log 8

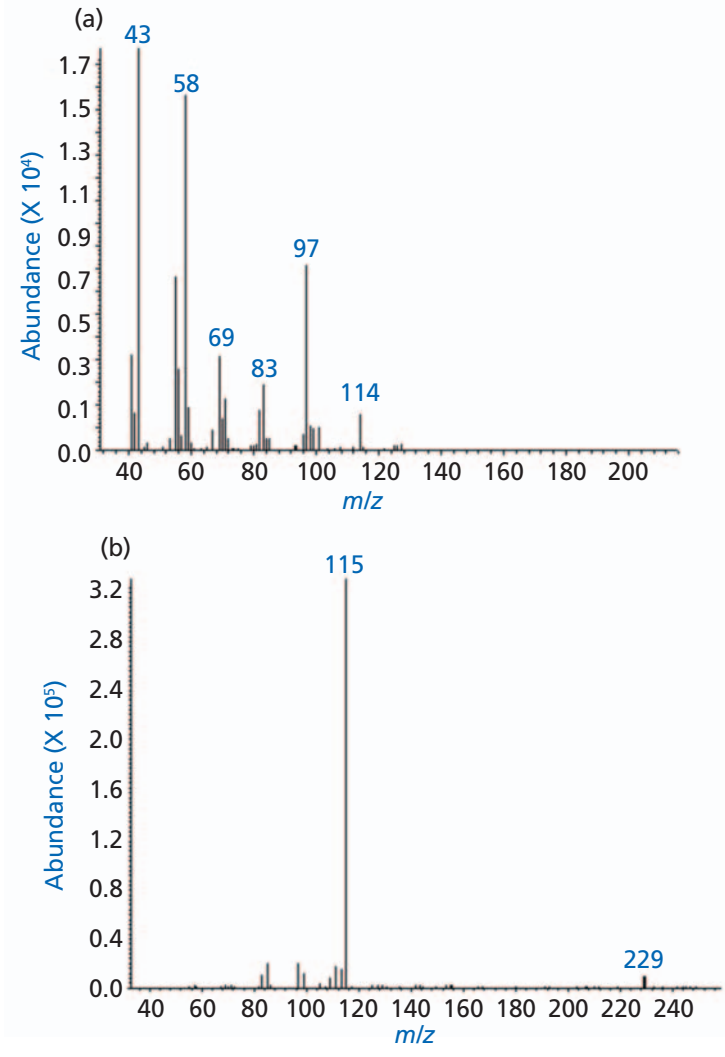

Figure 8: Mass spectra of a predominant peak in the TIC of fog oil: (a) EI, (b) CI.

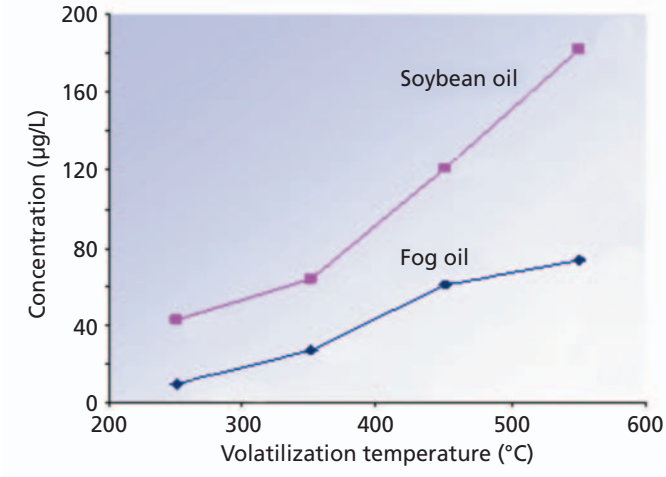

Figure 9: Aggregated concentration of volatile and semivolatile organics in the vapor stream of soybean oil and fog oil volatilized at different temperatures.

550 °C are shown in Figures 3a and 3b, respectively. Chromatograms show that oil volatilized at 550 °C yielded a higher number of volatile and semivolatile products than volatilization at 400 °C. Identification of the product peaks, where possible, was established through retention time match with known standard and EI mass spectra match when such matches were found in the library. In cases where the identity could not be established with reasonable certainty, CI spectra were used to enhance the certainty of identification. This approach was found to be useful in confirming the identity of short chain alkyl aldehydes and other analytes that did not yield an abundant molecular ion in the EI.

TICs obtained in the EI and CI mode showed essentially the same retention times and reasonable similarity in relative abundances of peaks. The EI and CI spectra of a dominant peak (marked with an asterisk *) in the TIC of soybean oil volatilized at 400 °C and 550 °C are shown in Figures 3a and 3b, respectively. The EI spectrum of the peak showed a very weak ion at *m/z* 100 and with fragment ions at *m/z* 44, 56, 72, and 82. The ion at 44 results from the classical γ hydrogen rearrangement followed by radical site initiated α cleavage as depicted in Figure 4a.

The CI spectrum of the same peak showed three predominant ions at *m/z* 83, 101, and 201, the pseudomolecular $(M+H)^+$ ion appeared at *m/z* 101, as shown in Figure 5b. The CI spectrum contain strong pseudomolecular ions and a strong fragment ion resulting from the loss of water as a neutral molecule, through γ hydrogen rearrangement followed by inductive cleavage and loss of water as a neutral species (Figure 4b). The ion at *m/z* 201 in the CI spectrum is most likely the adduct ion $[(M+H)+M]^+$ and the presence of this ion indicates that the analyte is present at high concentration, is indeed *n*-hexanal.

The EI and CI spectra of another strong peak in the TIC of soybean oil volatilized at 550 °C are shown in Figures 6a and 6b, respectively. The base ion in the EI spectrum was at ion *m/z* 41, the highest mass ion was observed at *m/z* 98. Other ions were observed at *m/z* 55, 69, and 83. The CI spectrum of the peak showed a single ion at *m/z* 99, the protonated pseudomolecular $(M+H)^+$. The peak is most likely that of 2-heptenal. Other peaks in the chromato-

gram were identified through this approach were found to be short and medium chain aldehydes and acids, including hexanal, heptanal, octanal, nonanal, hexanal, 2-hexenal, heptenal, propionic acid, hexanoic acid, heptanoic acid, and nonanoic acid.

The TICs of vapors formed during volatilization of mineral oil (fog oil, FO) under the same conditions used for soybean oil are shown in Figures 7a and 7b, respectively. Fog oil is a middle distillate petroleum product and it comprises a large number of branched chained hydrocarbons that are difficult to resolve, and chromatograms of such oils show a "hump." The hump is evident in both chromatograms. The chromatogram of oil volatilized at 550 °C showed higher numbers of volatile species (Figure 7b). The chromatogram of oil volatilized at 400 °C contained fewer volatiles. The identities of volatile and semivolatile compounds in the vapor stream was carried out through an analogous approach used in the case of volatiles generated with soybean oil.

The vapor stream resulting from volatilization of fog oil over the 400–550 °C temperature range was found to contain higher concentrations of ketones and alkenes. The EI spectra of the most predominant peak in the TIC of fog oil volatilized at 400 °C showed the presence of a weak ion at *m/z* 114, possibly the molecular ion and strong fragment ions at *m/z* 43 and 58 (Figure 8a). Such ions are characteristic of ketones—for example, the ion at *m/z* 43 most likely resulted from α-cleavage (Figure 5c) whereas the ion at *m/z* 58 resulted from γ-H rearrangement followed by α-cleavage (Figure 5d). The CI spectrum of the same peak showed a dominant ion at 115, most likely the pseudomolecular ion $(M+H)^+$. An adduct ion peak was also observed at *m/z* 229, most likely $(M+H+M)^+$ (Figure 8b). Thus, strong evidence for the presence of heptanone was provided.

The volatized fog oil stream also contained alkenes. The identities of analytes were quantified through internal standard normalized ion intensities obtained with the EI source. The predominant volatile and semivolatile compounds detected in the fog oil vapor streams were acetone, 2-pentanone, 2-hexanone, hexane, heptane, 2-heptanone, decane decene, and undecane. The fog oil stream contained lower concentrations of aldehydes and acids.

Comparisons of oxygenated molecules concentration and total volatiles obtained with different oils showed that concentrations of volatiles and antimicrobial activity were affected by two parameters: the composition of the starting material and the volatilization temperature. The results showed that volatilization temperature had a marked effect on the type and amount of total volatile components. Quantitative chemical characterization showed that production of the volatile species increased with an increase in temperature as long as the temperature was less than the combustion temperature; relative concentrations of volatile products obtained from fog oil and soybean oil over the volatilization temperature range is shown in Figure 9. The formation of volatile and semivolatile organics from other vegetable oils and monoesters showed a similar trend. Results showed that the composition of volatile and semivolatile organics produced during volatilization of oils is dependent on the chemical composition of oils, volatilization temperature, and volatilization atmosphere. The composition had a direct bearing on antimicrobial activity of the vapor stream. The antimicrobial activity of soybean oil and fog oil streams on vegetative *E. coli* are summarized in Table I.

Short- and medium-chain aldehydes and acids produced during volatilization of vegetable oil, such as soybean oil, act as highly effective antimicrobial agents and seem to support the assumptions made in ancient literature.

Conclusions

GC–MS characterization of volatile and semivolatile chemicals produced during rapid volatilization of oils at elevated temperatures results in the formation of an array of short- and medium-chain oxygenated molecules, including ketones, aldehydes, and acids. The formation depends on the oil being volatilized, the volatilization temperature, and the atmosphere. Higher yields are obtained from vegetable oils with a higher degree of unsaturation, such as the soybean oil. Yields are lower from petroleum oils such as mineral oil.

Oxygenated molecules, especially aldehydes and acids, act synergistically and show potent antimicrobial activities against a very wide variety of microbes including vegetative bacteria , bacterial spores, and fungal spores.

References

(1) World Health Organization, *Fact Sheet Antimicrobial Resistance (AMR)* (WHO, updated September 2016).

(2) D. Beatovic, D.K. Milosevic, S. Trifuovic, J. Siljegovic, J. Glamoclija, M. Ristic, and S. Jelacic, *Rec. Nat. Prod.* **9**(1), 62–75 (2015).

(3) A. Lius, D.M. Neiva, H. Pereira, J. Gominho, F. Domingues, and A.P. Duarte, *Ind. Crops Prod.* **91,** 97–103 (2016).

(4) Rigveda 1.72.3 (2000–1500 BCE).

(5) Atharvaveda 1.8.1 (1500–1000 BCE).

(6) E. Choe and D.B. Min, *Compr. Rev. Food Sci. Food Saf.* **5**(4), 169–186 (2006).

(7) C.H. Gertz, *Eur. J. Lipid Sci. Technol.* **102,** 543–551 (2000).

(8) A.K. Rani, S.Y. Reddy, and R. Chetana, *Eur. Food Res. Technol.* **230**(6), 803–811 (2010).

(9) J. Kamsiah and Y. Kamisah,in *Lipid Peroxidation*, A. Catala, Ed. (InTech Open, 2012), pp. 211–228.

(10) V.S. Rubalya, P. Neelanegam, and S.R. Vignesh, *Int. J. ChemTech Res.* **6**(11), 4671–4677 (2014).

(11) A.M. Ashaful, H.H. Majuki, M.A. Abul Kalam, R. Ashrafur, M. Habibullah, and M. Syazwan, *Energy and Fuels* **28**(2), 1081–1089 (2014).

(12) K.S. Snelson, R. Butler, R. Farlow, R. Welker, and S. Mainer, "Physical and Chemical Characterization of Military Smokes" Fog oils and oil fogs InstituteDAMD17-787-8085. ADA093205. IIT Research Institute, Chicago, IL. (US Army Technical Report, 1980).

(13) K. Stackleberg, C. Amos, T. Smith, D. Cropek, and B. MacAllister, "Military Smokes and Obscurants – Fate and Effects," ERDC/CERL TR-04-29, (US Army Technical Report, 2004) US Army Corps of Engineers.

Racha Seemamahannop and Shubhen Kapila are with the Department of Chemistry at Missouri University of Science and Technology in Rolla, Missouri. **Prakash Wadhawa** is with the Department of Chemical Engineering at Missouri University of Science and Technology. **Abha Malhotra** is with the History Department at Himachal University in Shimla, Himachal Pradesh, India. Direct correspondence to: kapilas@mst.edu ■

Mass Spectrometry Techniques to Unravel the Heterogeneity of Glycoproteins

The production of high-quality pharmaceutical recombinant therapeutic glycoproteins with consistency in glycan quality is still challenging. Since glycans are responsible for bioactivity, solubility, immunogenicity, and clearance rate from circulation, it is vital to have a detailed map of glycans in therapeutic glycoproteins. Detailed glycoprotein structural analysis must be able to identify the peptide sequence where the glycans are attached as well as the structure of the glycan portion, including oligosaccharide sequence and glycosyl linkages. We detail methods for mass spectrometry (MS) experiments on both released glycans ("glycomics"), as well as on intact glycopeptides ("glycoproteomics") using electron transfer dissociation (ETD), high-energy collision dissociation (HCD), and collision-induced dissociation (CID) fragmentation pathways, which are needed to fully elucidate the structure of glycoproteins. We also show additional protocols of a combination of glycosyl composition and glycosyl linkage analysis, using a combination of methylation analysis, multiple-stage mass spectrometry (MS^n), and exoglycosidase digestion, and provide information on the glycan topology as well as detection methods for potential nonhuman modifications that could arise from mammalian expression systems such as Galα1-3Gal and *N*-glycolylneuraminic acid (NeuGc). Our consolidated experiments outline all the necessary information pertaining to the glycoprotein, including glycan fine structure, attachment site, and glycosylation degree to be obtained for pharmaceutical recombinant glycoproteins.

Asif Shajahan and Parastoo Azadi

At least half of all proteins in living organisms are glycosylated, so the importance of structural characterization of glycoproteins is increasing rapidly (1). Glycans directly or indirectly influence many cellular physiological functions, and the study of precise glycan structure, their structural variability, their sites of attachment to the protein, and the degree to which these sites are occupied are vital in deducing their functional roles. Nontemplate-driven biosynthesis and microheterogeneity of glycosylation often make the structural assignment tasks difficult (2). A set of glycosyltransferases drives the biosynthesis of glycans, and glycans on a glycosylation site exist as mixtures of heterogeneous structures. Structural determination of carbohydrates from complex biological samples are most commonly determined by analytical techniques using electrospray ionization mass spectrometry (ESI-MS), matrix-

assisted laser desorption–ionization MS (MALDI-MS), capillary electrophoresis (CE), and nuclear magnetic resonance (NMR) spectroscopy (3). The composition of monosaccharides in glycans and their branching is determined by MS, whereas gas chromatography (GC) (after chemical derivatization) or NMR is used for the determination of linkage information and monosaccharide types. These complementary techniques are often required to be used together for the comprehensive determination of glycosylation (4,5). MS is one of the major techniques for the analysis of glycoproteins that are usually available as a heterogenic mixture in minute amounts since it can, in principle, be used for the analysis of complex mixtures of samples of low abundance. Mammalian glycans, which consist of a limited assortment of monosaccharides, are often isomeric, having the same molecular mass. The glycans are usually multiply branched and exist as mixtures of various branching and substitution patterns (6). Since numerous potential attachment points exist in each monosaccharide, multitudes of isomeric structures are possible. Stereoisomers such as mannose and galactose, which are not quite distinct based on their molecular mass, produce a slightly different ring cleavage pattern in tandem multiple-stage mass spectrometry (MS^n) analysis. Thus, analytical techniques such as glycosyl linkage or composition analysis by GC–MS of partially methylated alditol acetates (PMAAs) generated from glycans are performed to distinguish stereoisomers (7). Glycans that are found on the cells in the form of either glycoproteins or glycolipids are covalently linked to proteins or lipids, respectively. The linkages between two monosaccharides are called *glycosidic bonds* and the linkages between glycans and proteins are classified as either N-linked or O-linked. In N-linked glycans, the linkage between glycan and protein is through the side chain nitrogen of asparagine. On the other hand, glycans involving linkage through the side-chain oxygen of serine or threonine of peptides are O-linked glycans (Figure 1) (6).

MALDI-time-of-flight (TOF) MS is one of the most common techniques used for glycan characterization, and it enables rapid and sensitive analyses of singly charged larger biomolecules (8). Because of the structural complexity and low ionization efficiency of carbohydrates that results from their hydrophilicity, MALDI-TOF MS analyses are usually performed after the permethylation of glycans, which improves their sensitivity for MS detection by increasing the ionization efficiency of glycans up to 20-fold (9). Other complementary techniques such as ESI-MS and MS^n fragmentation enable further structural characterization of selected glycan ions, and that helps in the differentiation of "isobaric" glycans, which have the same mass but different sugar compositions, linkages, or structures (10). Liquid chromatography–tandem mass spectrometry (LC–MS/MS) analysis of permethylated glycans assists in obtaining the structural determina-

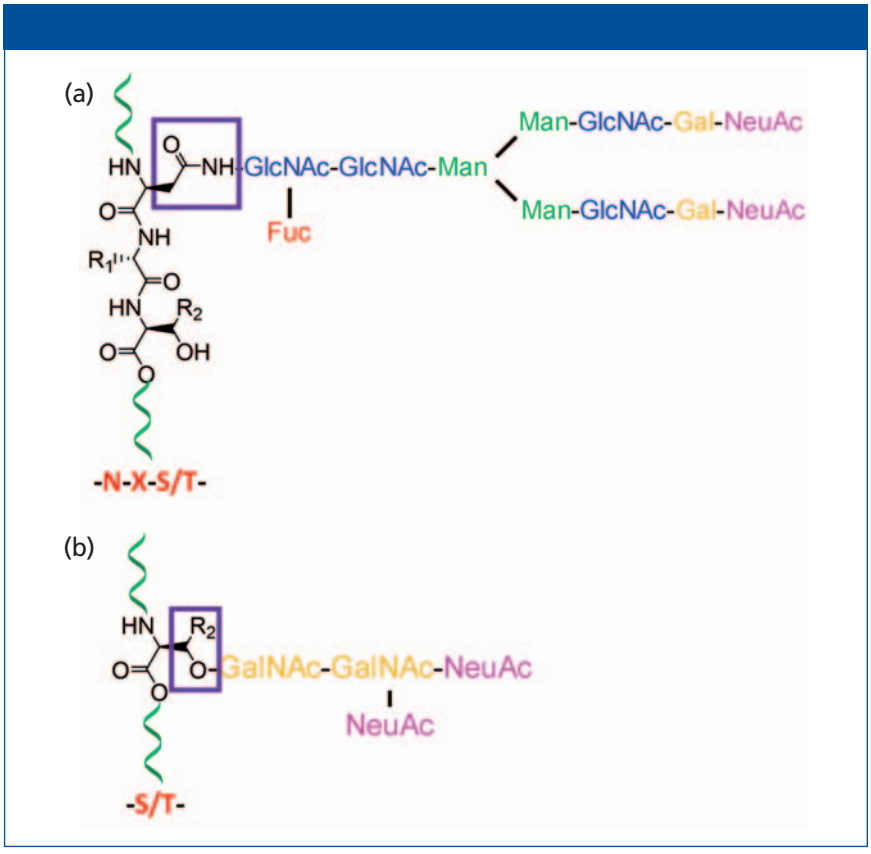

Figure 1: Typical structure of protein glycosylations that are classified into (a) N-linked glycans where glycans are attached to the side chain of asparagines (N) on N-glycan consensus sequence NXS/T; and (b) O-linked glycans where glycans are attached to either serines or threonines of proteins.

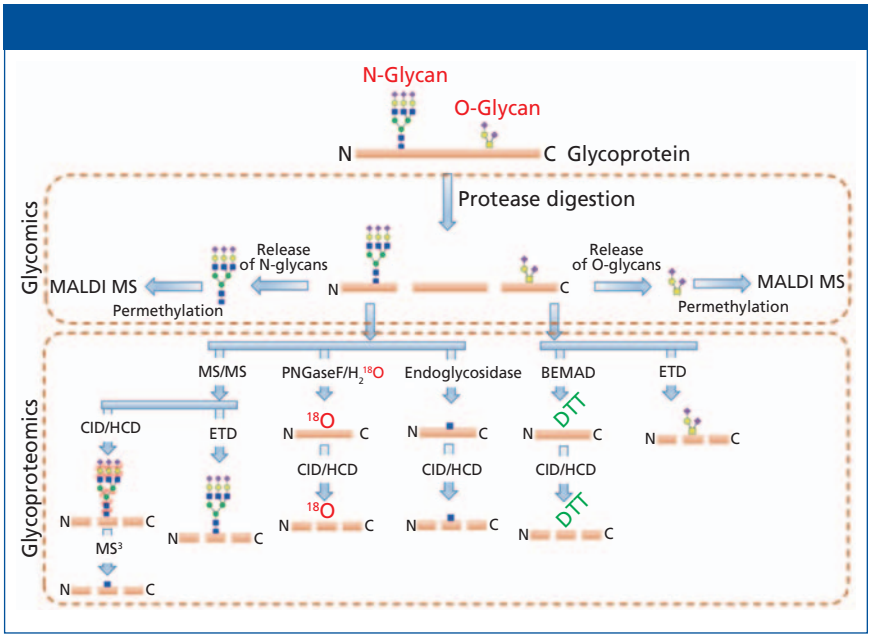

Figure 2: MS-based techniques used to determine the N- and O-linked glycosylation (PTM) on glycoproteins by glycomics and glycoproteomics.

tion of isomers and further selective fragmentation. Recently, better chromatographic separation and trapped ion mobility spectrometry (TIMS) was used for the characterization of isomeric glycans (10,11).

This article is intended to provide a brief overview of the general techniques involved in the characterization of heterogeneous glycoproteins, such as the determination of glycan structure, sites of glycosylation, site-specific glycan heterogeneity, and glycosylation site occupancy of glycoproteins using MS.

Determination of Protein Glycosylation by MS

Comprehensive analysis of the cellular glycan repertoire is essential for the study of underlying mechanisms in complex biological processes such as intra- and intercellular signaling, organ development, immunological responses, tumor growth, and even stability of bioconjugates. When the structural analysis of protein glycosylation is performed with the released glycans, the approach is termed *glycomics*. On the other hand, the analysis of glycosylation on proteins without its release is termed as *glycoproteomics* (Figure 2). The most common analytical procedures for the characterization of glycosylation comprise the analysis of the individual glycan structures in detail along with their isomeric pattern (glycomics) and detailed evaluation of site of glycosylation on glycoproteins and glycopeptide characterization (glycoproteomics), including the glycan variability and degree of occupancy of the site (6,12).

The analysis of glycoproteins is often challenging because of several factors such as relatively poor ionization of glycopeptide with respect to the peptide, the presence of heterogenous glycan isomers (glycoforms), the lack of a comprehensive database of glycan structures (including microbial and plant derived structures), and the lack of MS signature fragment ions for the complete structure determination. Even though a number of bioinformatics tools are currently available for glycomics and glycopeptide analysis, accurate determination of highly heterogeneous glycan attachment on peptides is still a challenging task (8,13). Thus, the samples are currently split into two separate workflows for the comprehensive characterization of glycan structure on glycoproteins via glycomic and glycoproteomic analysis. Glycoproteins are first proteolytically cleaved to obtain

peptides and glycopeptides. The protease digest is directly used for glycoproteomic analysis by injecting to a LC–MS/MS system with or without enrichment. Proteolysis is also performed for glycomic analysis as a preliminary step before the enzymatic release of N-glycans since the glycan release is more efficient from glycopeptides than from intact or denatured glycoproteins because of the decreased steric hindrance (14,15). Nonhuman modifications, such as Galα1-3Gal and *N*-glycolylneuraminic acid (NeuGc), that could arise from mammalian expression systems can also be determined by both glycomics and glycoproteomics analysis.

Glycomics Analysis

Glycomics analysis enables the introduction of analytes directly into the MS instrument, so multiple MS fragmentation of the analyte ions is possible. Moreover, glycomics allows derivatization of molecules with chromophores, fluorophores, and permethylation, making them more suitable for further downstream analysis techniques such as high performance liquid chromatography (HPLC), NMR, and MS (Figure 2) (16). For the glycomics analysis of glycoproteins, glycans are released by either enzymatic or chemical treatment, depending on the type of glycans being released. N-Glycans are usually released from the glycopeptides using N-glycanase enzymes—for example, either PNGase F or PNGase A, which cleaves the N-linked glycans from the peptide asparagines (17).

The hydrophilic released N-glycans are separated from the peptides and O-linked glycopeptides using a C18 solid-phase extraction (SPE) cartridge or nonporous graphitized carbon column (18). The separated N-glycans are further derivatized based on the downstream analytical technique used for their characterization. The releasing of an O-glycan is usually conducted using chemical methods such as reductive β-elimination, ammonia-based nonreductive β-elimination, or hydrazinolysis since deglycosylation enzymes with wide specificity for O-linked glycans are not available (14,19,20). Similar to N-glycans, released O-linked glycans are also derivatized before downstream analysis, either by permethylation or by reducing-end labeling with chromophores such as 2-aminobenzamide (2-AB), 2-aminopyridine (2-AP), 4-aminobenzoic acid, or anthranilic acid (21).

Derivatization enhances the ionization efficiency of the released glycans, and permethylation is the most popular mode of glycan derivatization because it enables detailed structural information of glycans by MS^n through both glycosidic and cross-ring cleavages (Figure 3) (22). Moreover, the permethylated glycans can also be further manipulated and used for the determination of glycosylation linkages by GC–MS. For the linkage determination, the permethylated glycans are acid-hydrolyzed, reduced, acetylated, and the resulting PMAAs are analyzed by GC–MS (7).

To quantitate the monosaccharide composition of glycans, monosaccharides derived from glycans by acidic methanolysis were derivatized by tri-

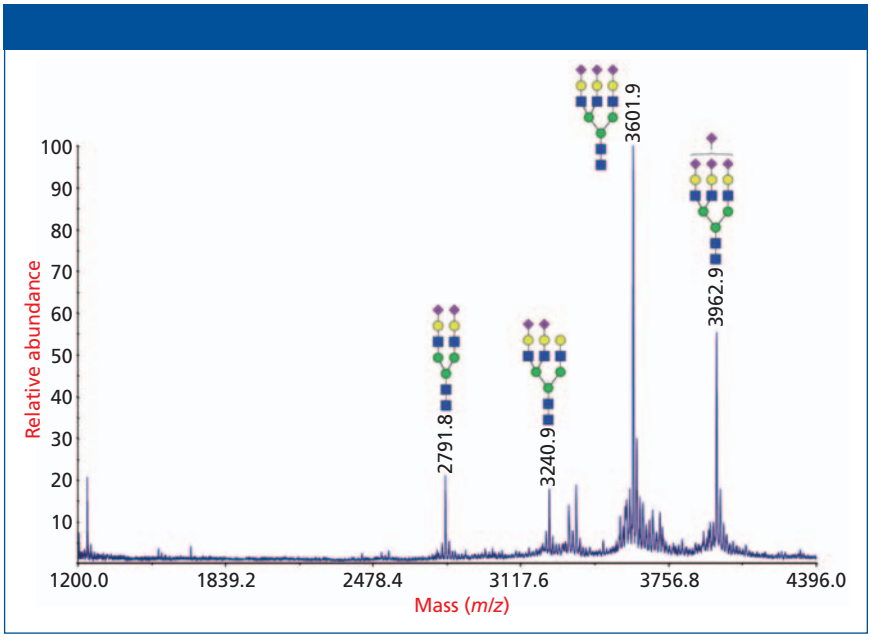

Figure 3: Analysis of N-glycans from bovine fetuin by glycomics analysis. N-glycans were released from the glycoprotein by PNGase F, permethylated and analyzed by MALDI-TOF-MS.

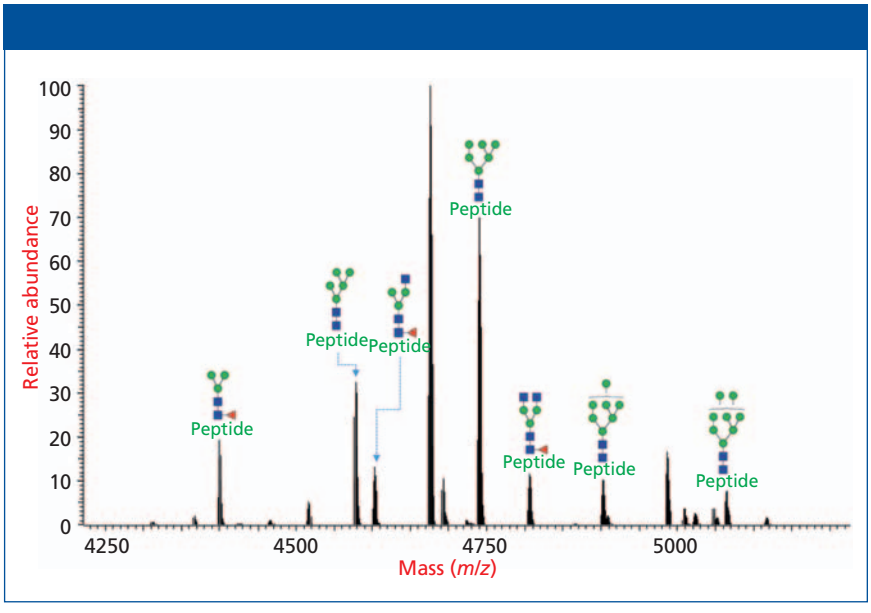

Figure 4: Glycoforms of N-linked glycosylated peptide determined by glycoproteomics analysis where the protease digest of the glycoprotein is injected to an LC–MS/MS system and analyzed via HCD–CID fragmentation.

methylsilyl (TMS) groups and analyzed by GC–MS (23). The monosaccharide composition analysis is also determined by high-performance anion exchange chromatography with pulsed amperometric detection (HPAEC-PAD) of monosaccharides released from the glycans by acid hydrolysis (24).

One of the major drawbacks of the glycomics approach is that the site-specific information of glycosylation, such as the attachment site and occupancy rates, is lost since the glycans are released from the protein. Attempts to perform detailed structural characterization of glycans while keeping the glycan point of attachment to the protein intact are gaining a lot of attention from researchers recently because that analysis simplifies the current multi-step analytical procedure used for the characterization of glycosylations.

Glycoproteomics Analysis

The glycans are not released in the glycoproteomics approach and the glycan-peptide bonds are kept intact to obtain information about glycosylation sites and site occupancies. The analysis of intact glycopeptides by LC–MS/MS is the most popular method for the rapid determination of glycosylation at specific site of peptides (Figure 4). Glycoproteomic analysis consists of glycosylation site mapping and determination of the composition of glycans attached at each site (Figures 2, 4, 5, and 6) (17).

The glycoproteins are digested into smaller peptides and glycopeptides using proteases and the resulting protease digest is injected directly to an LC–MS/MS system. The peptides and glycopeptides fractionated by the LC system is injected to a high-resolution MS instrument and their precursor mass along with the mass of ions after MS fragmentations are analyzed.

Site mapping reveals the potential glycosylation sites that are occupied and this information is useful for subsequent glycopeptide analysis. Analytical challenges associated with determining the glycosylation site from intact glycopeptides is the lack of adequate peptide fragmentation during MS/MS, thus performing analysis on deglycosylated peptides or partially deglycosylated peptides is required. One of the common techniques for deglycosylation is the enzymatic removal of N-linked glycans with peptide-N-glycosidase (PNGase) in ^{18}O-labeled water (Figure 5a) or partial enzymatic degradation of the N-linked structures using endo-β-*N*-acetylglucosaminidase (17,25). However, the sites of O-linked glycans can be determined without releasing them since O-glycans are usually smaller in size; peptide fragmentation by a non-ergodic fragmentation approach such as electron transfer dissociation (ETD) can be used for the site determination (Figure 6). Ergodic fragmentation techniques, such as collision-induced dissociation (CID) fragmentation or high energy collisional fragmentation (HCD), will lead to fragmentation of the peptide–glycan bond preferentially, so they are not ideal for the site map-

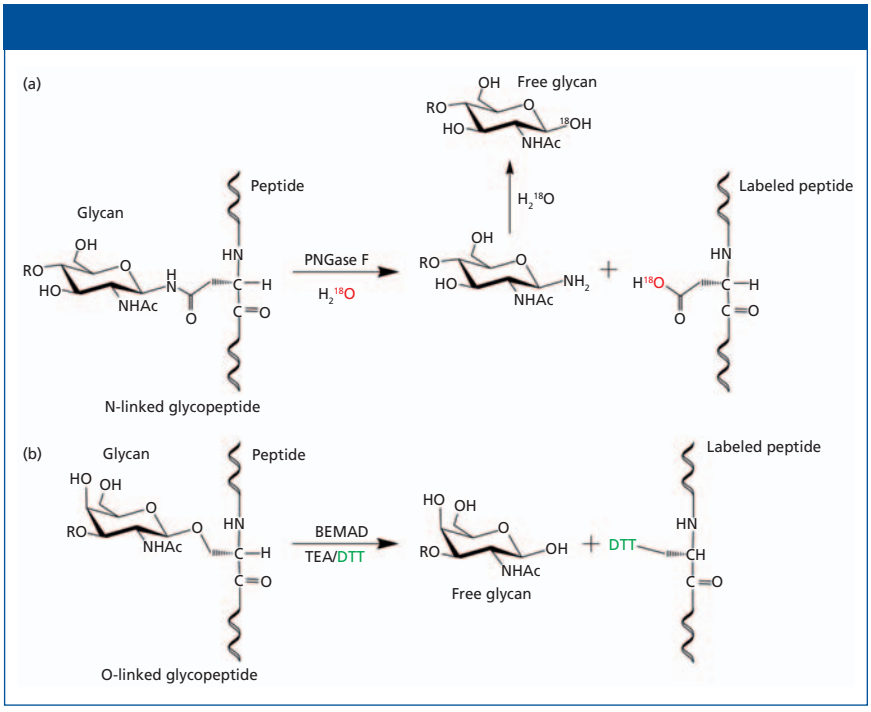

Figure 5: Site determination of (a) N-linked glycosylation through ^{18}O labeling by deglycosylation using PNGase F in $H_2{}^{18}O$; (b) O-linked glycosylation through DTT labeling via BEMAD reaction (TEA: triethylamine, DTT: dithiothreitol).

ping of O-linked glycopeptides (Figure 7). Moreover, for the site mapping of glycoproteins carrying large or heavily glycosylated (that is, mucin), the removal of O-linked glycans may be required (17). An approach to accomplish the release of O-glycans with simultaneous site-labeling termed *β-elimination by Michael addition with dithiothreitol* (*BEMAD*) is also used for site mapping in which a mildly alkaline β-elimination in the presence of dithiothreitol (DTT) is performed (Figure 5b) (26).

Glycopeptides or deglycosylated and labeled peptides are analyzed by MS (that is, MALDI-TOF MS or ESI-MS) directly or through LC–MS/MS. For the LC–MS/MS analysis, the peptides, glycopeptides, or labeled peptides are first separated on a LC and then injected online into a high-resolution MS system for the mass analysis of intact and fragmented peptide–glycopeptide ions. Information about both the glycans and their attachment sites is obtained from the glycoproteomics data. However, comprehensive characterization of glycans attached on each site is accomplished by the glycomics.

The information about the type of glycans through the glycomic analysis and the site mapping data helps for the accurate and easy glycoproteomic data analysis by narrowing the range of possible masses to look for from the LC–MS/MS data (22). One of the most crucial steps in both glycomics and glycoproteomics analysis is the data interpretation from multiple types of tandem MS^n and LC–MS/MS data. Various bioinformatics tools comprising several databases curated through experimental data, an in-silico fragmentation prediction tool, search algorithms, annotation tools, and glycan structure drawing tools are used for the determination of glycosylation on glycoproteins (27–29).

Recent Advances in Glycomics and Glycoproteomics

The complexity and microheterogeneity of glycosylation and the discovery of novel glycosylation from prokaryotes demands methodological progress in the techniques used for the structural characterization of glycoproteins.

Considerable advances have been made recently for the MS analysis of glycoproteins including novel sample preparation techniques such as frac-

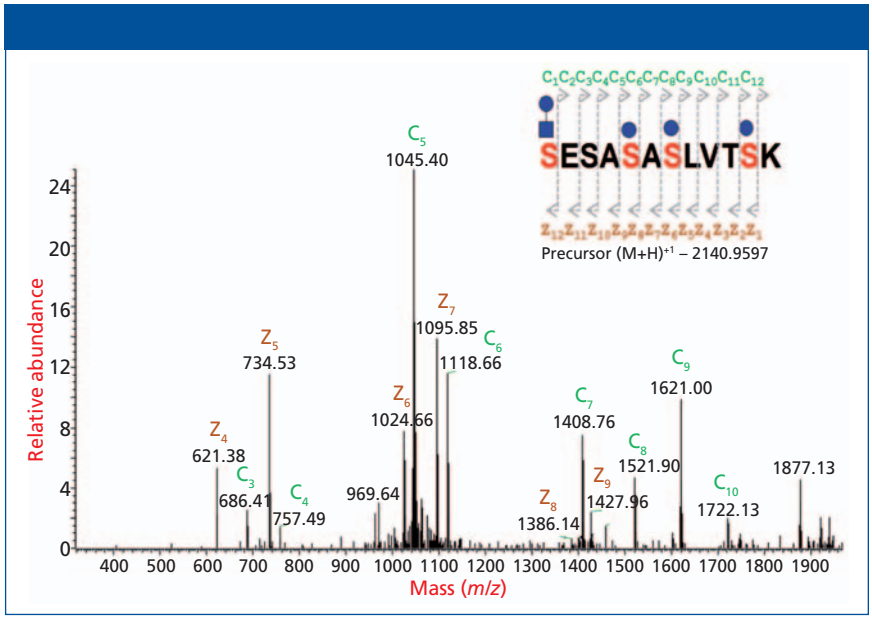

Figure 6: Site mapping of O-glycosylation by ETD MS^2 of glycopeptide. The exact location of glycosylation can be mapped from the c and z ion fragments of the ETD spectrum.

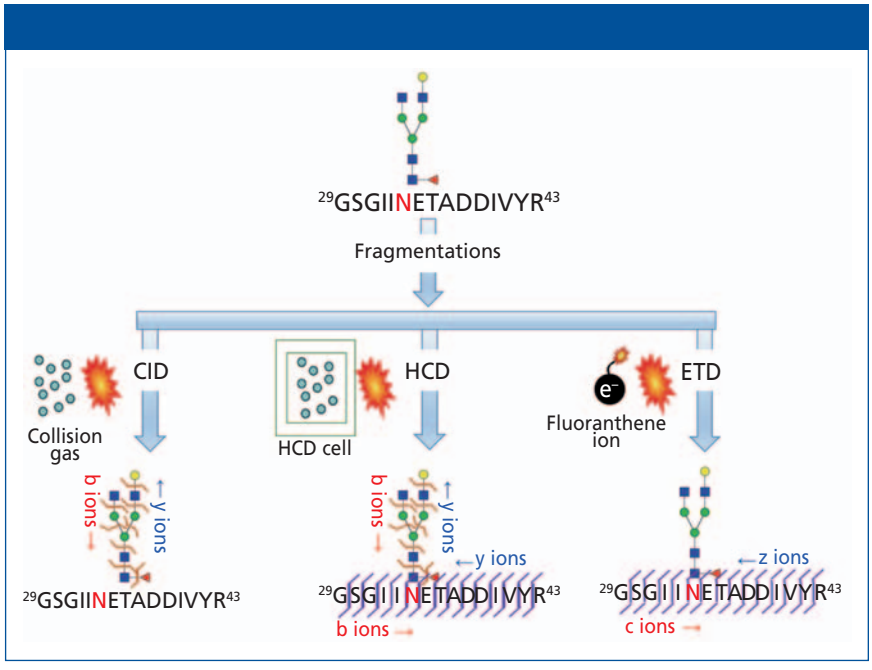

Figure 7: Glycopeptides are analyzed by tandem MS fragmentations. CID provides information on the glycan portion, HCD provides information on glycan portion and partial information on peptide sequence, and ETD provides the site of glycosylation information.

tionation, preconcentration; quantitation techniques, such as the use of label-free and isotopic-labeling methods; and instrumentation methods such as ion mobility mass spectrometry (IM-MS) and the flexible use of fragmentation modes. Researchers are increasingly focusing on the quantitative analysis of glycoproteins, in addition to the qualitative data (17).

Better and robust software and computer aided tools were developed recently for the data analysis of highly complex and enormous data volumes obtained through these modern techniques. Volumetric and sampling errors were reduced, and overall reproducibility and analytical throughput were improved by automating the individual steps in glycomics and glycoproteomics. Nevertheless, because of the highly heterogenous nature and presence of very low levels in comparison to cellular proteomes, a comparison of "normal" versus "aberrant" glycosylation levels of complex glycans from various sources is still challenging (30). Glycoprotein characterization using a 96-well plate format via multistep procedures including protein denaturation, deglycosylation, desialylation, permethylation, and subsequent MALDI-MS profiling, were recently achieved successfully (31). Moreover, glycan derivatizations before MS analysis were also automated recently, with very good reproducibility (32). Recently, the permethylation protocol was automated and high-throughput analysis for the glycan profiling of monoclonal antibodies and recombinant human erythropoietin was conducted using robotics (33).

Currently, wide-ranging databases of anti-glycan reagents, such as lectins and antibodies, are available and commercial availability of these reagents for glycoprotein fractionation and glycan-epitope detection have been increased progressively (34–36).

Several recent studies addressed the shortcomings of chemical and enzymatic release of glycans by the development of new chemical glycan release methods (37–39), immobilization of PNGase F (40), optimization of PNGase F release of N-glycans (41), discovery of broad substrate-specific N-glycosidases (42), and high-throughput glycan releasing (30).

Hydrophilic-interaction chromatography (HILIC) HPLC hyphenated with fluorescence detection of reductively aminated glycans with fluorescent tags is the most widely used technique for glycan quantification in the pharmaceutical industry, and the procedure can be validated easily under good manufacturing practice (GMP) regulations. Various recent advances were reported on the development of better HILIC-based separation techniques for the improved isomeric separation of glycans (43–45). Derivatization of glycans with a fluorophore has several advantages, such as enhanced sensitivity of analysis with both spectroscopic and MS detectors and increased hydrophobicity of glycans, thereby increasing their chromatographic retention in

reversed-phase LC. A newly reported label, RapiFluorMS (RFMS), enables rapid labeling of released N-glycans at their reducing end. The label bears a quinone moiety as fluorophore and a tertiary amine for strong positive-mode ionization (46).

Much attention has recently shifted in the field of glycomics and glycoproteomics toward quantitative estimation in which MS-based relative and absolute quantification of glycoconjugates is performed. Labeling the analyte with an isotope tag is the most common method for MS-based relative quantitation since the isotope tag does not interfere with chromatography and ionization in MS and provides an isotopic mass shift to distinguish the labeled molecules (47). For the estimation of relative quantity, "light" and "heavy" isotope-labeled glycans, in which isotopic tags with lower mass and higher mass are used, respectively, are mixed at different ratios, and the corresponding MS peak intensity is compared (48).

Even though MALDI and ESI are the most common modes of ionization in glycan and glycopeptide characterization, each of them have their own disadvantages. ESI-MS has the disadvantage of in-source fragmentation, which leads to misinterpretation and poor sensitivity. Several new technologies were developed recently to address these limitations; notably, subambient pressure ionization with a nano-electrospray (SPIN) source was developed in which the ESI emitter was moved to the first vacuum stage of the mass spectrometer at the entrance of the electrodynamic ion funnel to enhance the collection of the entire electrospray plume (49). To optimize the collision energy required for the fragmentation, stepping of CID collision energy that allows simultaneous acquisition of MS/MS spectra of glycopeptide at lower and higher collision energies was developed (50).

Since the glycopeptide MS data interpretation is typically challenging and the false discovery rates (FDR) need to be reduced, intelligent data-dependent decision trees of sequential fragmentation steps of glycopeptides like HCD-product-dependent ETD and CID workflows using orbital ion trap mass spectrometers were developed recently. Such improved MS/MS data and several newly developed data analyzing programs and search engines facilitated data interpretation (30,51).

Other recent developments in the charaterization of glycoproteins include the following advances: improved spectral data of glycans provided by the introduction of novel fragmentation methods such as ultraviolet photodissociation (UVPD) (52), the development of IM-MS and the application of it in the discrimination of linkage and position isomers, glycosylation site identification, the identification of α-2-3 and α-2-6 linked sialic acid linkage isomers (53), and the use of capillary zone electrophoresis for the efficient separation, resolution, and sensitivities in the analysis of glycoconjugates (32). Furthermore, an initiative termed *minimum information required for a glycomic experiment* (*MIRAGE*) was established in 2011 to promote critical evaluation of experimental protocols, dissemination of data sets for reproducibility, and comparison of results obtained in different laboratories (54).

Summary

Considerable advances were observed during the past decade for the analysis of glycoproteins. The demand for the identification and characterization of the glycome associated with proteins is increasing since the role that protein glycosylation plays in cellular physiology and disease processes is being increasingly deduced. The discovery of novel disease biomarkers, characterization of recombinant glycoprotein therapeutics, the study of the roles of glycosylation on cell signaling and immunology, and microbial and plant glycobiology are the most important fields in which the structural characterization of glycoconjugates is required.

This article has emphasized the most common techniques involved in the interpretation of glycan structure on glycoproteins and also highlighted the recent progress in the field of glycoprotein analysis by mass spectrometry. Advancements in the analytical procedures in glycomics and glycoproteomics would enable rapid yet comprehensive characterization of highly heterogenous glycomes.

Acknowledgments

This work was supported in part by National Institutes of Health (NIH)-funded Research Resource for Biomedical Glycomics (S10OD018530, P41GM103490, R21GM122633) and the Chemical Sciences, Geosciences and Biosciences Division, Office of Basic Energy Sciences, U.S. Department of Energy grant (DE-SC0015662) at the Complex Carbohydrate Research Center.

Conflict of Interest Statement

The authors work at the Analytical Services & Training Laboratory at the Complex Carbohydrate Research Center at the University of Georgia and perform glycomics and glycoproteomics analysis as collaboration or fee-for-service.

References

(1) R. Apweiler, H. Hermjakob, and N. Sharon, *Biochim. Biophys. Acta* **1473,** 4–8 (1999).

(2) R.D. Astronomo and D.R. Burton, *Nat. Rev. Drug Discov.* **9,** 308–324 (2010).

(3) R. Raman, S. Raguram, G. Venkataraman, J.C. Paulson, and R. Sasisekharan, *Nat. Methods* **2,** 817–824 (2005).

(4) M. Guerrini, R. Raman, G. Venkataraman, G. Torri, R. Sasisekharan, and B. Casu, *Glycobiology* **12,** 713–719 (2002).

(5) G. Venkataraman, Z. Shriver, R. Raman, and R. Sasisekharan, *Science* **286,** 537–542 (1999).

(6) A. Varki, R.D. Cummings, J.D. Esko, P. Stanley, G. Hart, M. Aebi, A. Darvill, T. Kinoshita, N.H. Packer, J.J. Prestegard, R.L. Schnaar, and P.H. Seeberger, in *Essentials of Glycobiology,* 3rd Edition (Cold Spring Harbor, New York, 2015).

(7) W. Morelle and J.C. Michalski, *Nat. Protoc.* **2,** 1585–1602 (2007).

(8) M. Wuhrer, M.I. Catalina, A.M. Deelder, and C.H. Hokke, *J. Chromatogr. B Analyt. Technol. Biomed. Life Sci.* **849,** 115–128 (2007).

(9) D.J. Harvey, *Mass Spectrom. Rev.* **18,** 349–450 (1999).

(10) C.E. Costello, J.M. Contado-Miller, and

J.F. Cipollo, *J. Am. Soc. Mass Spectrom.* **18,** 1799–1812 (2007).
(11) Y. Pu, M.E. Ridgeway, R.S. Glaskin, M.A. Park, C.E. Costello, and C. Lin, *Anal. Chem.* **88,** 3440–3443 (2016).
(12) H. Ito, H. Kaji, A. Togayachi, P. Azadi, M. Ishihara, R. Geyer, C. Galuska, H. Geyer, K. Kakehi, M. Kinoshita, N.G. Karlsson, C. Jin, K. Kato, H. Yagi, S. Kondo, N. Kawasaki, N. Hashii, D. Kolarich, K. Stavenhagen, N.H. Packer, M. Thaysen-Andersen, M. Nakano, N. Taniguchi, A. Kurimoto, Y. Wada, M. Tajiri, P. Yang, W. Cao, H. Li, P.M. Rudd, and H. Narimatsu, *Glycoconj. J.* **33,** 405–415 (2016).
(13) L. Cao, Y. Qu, Z. Zhang, Z. Wang, I. Prytkova, and S. Wu, *Expert Rev. Proteomics* **13,** 513–522 (2016).
(14) W.R. Alley, Jr. and M.V. Novotny, *Annu. Rev. Anal. Chem.* **6,** 237–265 (2013).
(15) Z. Szabo, A. Guttman, and B.L. Karger, *Anal. Chem.* **82,** 2588–2593 (2010).
(16) Y. Wada, A. Dell, S.M. Haslam, B. Tissot, K. Canis, P. Azadi, M. Backstrom, C.E. Costello, G.C. Hansson, Y. Hiki, M. Ishihara, H. Ito, K. Kakehi, N. Karlsson, C.E. Hayes, K. Kato, N. Kawasaki, K.H. Khoo, K. Kobayashi, D. Kolarich, A. Kondo, C. Lebrilla, M. Nakano, H. Narimatsu, J. Novak, M.V. Novotny, E. Ohno, N.H. Packer, E. Palaima, M.B. Renfrow, M. Tajiri, K.A. Thomsson, H. Yagi, S.Y. Yu, and N. Taniguchi, *Mol. Cell Proteomics* **9,** 719–727 (2010).
(17) A. Shajahan, C. Heiss, M. Ishihara, and P. Azadi, *Anal. Bioanal. Chem.* **409,** 4483–4505 (2017).
(18) Y. Li, J. Fu, Y. Ling, T. Yago, J.M. Mcdaniel, J. Song, X. Bai, Y. Kondo, Y. Qin, C. Hoover, S. Mcgee, B. Shao, Z. Liu, R. Sonon, P. Azadi, J.D. Marth, R.P. Mcever, C. Ruan, and L. Xia, Proc. Natl. Acad. Sci. U. S. A. **114,** 8360–8365 (2017).
(19) I. Turyan, X. Hronowski, Z. Sosic, and Y. Lyubarskaya, *Anal. Biochem.* **446,** 28–36 (2014).
(20) R.P. Kozak, L. Royle, R.A. Gardner, D.L. Fernandes, and M. Wuhrer, *Anal. Biochem.* **423,** 119–128 (2012).
(21) D.J. Harvey, *J. Chromatogr. B Analyt. Technol. Biomed. Life Sci.* **879,** 1196–1225 (2011).
(22) W.R. Alley, Jr., B.F. Mann, and M.V. Novotny, *Chem. Rev.* **113,** 2668–2732 (2013).
(23) J. Bleton, P. Mejanelle, J. Sansoulet, S. Goursaud, and A. Tchapla, *J. Chromatogr. A* **720,** 27–49 (1996).
(24) M.R. Hardy and R.R. Townsend, *Methods Enzymol.* **230,** 208–225 (1994).
(25) B. Kuster and M. Mann, *Anal. Chem.* **71,** 1431–1440 (1999).
(26) L. Wells, K. Vosseller, R.N. Cole, J.M. Cronshaw, M.J. Matunis, and G.W. Hart, *Mol. Cell Proteomics* **1,** 791–804 (2002).
(27) M. Bern, Y.J. Kil, and C. Becker, *Curr. Protoc. Bioinformatics* Chapter 13, Unit13 20 (2012).
(28) A. Ceroni, K. Maass, H. Geyer, R. Geyer, A. Dell, and S.M. Haslam, *J. Proteome Res.* **7,** 1650–1659 (2008).
(29) M. Eavenson, K.J. Kochut, J.A. Miller, R. Ranzinger, M. Tiemeyer, K. Aoki, and W.S. York, *Glycobiology* **25,** 66–73 (2015).
(30) S. Gaunitz, G. Nagy, N.L.B. Pohl, and M.V. Novotny, *Anal. Chem.* **89,** 389–413 (2017).
(31) M.R. Bladergroen, K.R. Reiding, A.L.H. Ederveen, G.C.M. Vreeker, F. Clerc, S. Holst, A. Bondt, M. Wuhrer, and Y.E.M. Van Der Burgt, *J. Proteome Res.* **14,** 4080–4086 (2015).
(32) L.R. Ruhaak, C.a.M. Koeleman, H.W. Uh, J.C. Stam, D. Van Heemst, A.B. Maier, J.J. Houwing-Duistermaat, P.J. Hensbergen, P.E. Slagboom, A.M. Deelder, and M. Wuhrer, *Plos One* **8,** e73082 (2013).
(33) A. Shubhakar, R.P. Kozak, K.R. Reiding, L. Royle, D.I. Spencer, D.L. Fernandes, and M. Wuhrer, *Anal. Chem.* **88,** 8562–8569 (2016).
(34) S. Fanayan, M. Hincapie, and W.S. Hancock, *Electrophoresis* **33,** 1746–1754 (2012).
(35) Y.L. Hu, S.Y. Zhou, C.Y. Yu, H.X. Tang, and Y. Mechref, *Rapid Commun. Mass Spec.* **29,** 135–142 (2015).
(36) M.J. Kailemia, L.R. Ruhaak, C.B. Lebrilla, and I.J. Amster, *Anal. Chem.* **86,** 196–212 (2014).
(37) W.X. Chen, J.M. Smeekens, and R.H. Wu, *J. Proteome Res.* **13,** 1466–1473 (2014).
(38) X.Z. Song, H. Ju, Y. Lasanajak, M.R. Kudelka, D.F. Smith, and R.D. Cummings, *Nat. Methods* **13,** 528–534 (2016).
(39) X.Z. Song, H. Ju, C.M. Zhao, and Y. Lasanajak, *Bioconjugate Chem.* **25,** 1881–1887 (2014).
(40) M. Szigeti, J. Bondar, D. Gjerde, Z. Keresztessy, A. Szekrenyes, and A. Guttman, *J. Chromatogr. B* **1032,** 139–143 (2016).
(41) Y.J. Weng, Z.G. Sui, H. Jiang, Y.C. Shan, L.F. Chen, S. Zhang, L.H. Zhang, and Y.K. Zhang, *Sci Rep-Uk* **5,** 9770 (2015).
(42) Y.M. Du, T. Xia, X.Q. Gu, T. Wang, H.Y. Ma, J. Voglmeir, and L. Liu, *J. Agr. Food Chem.* **63,** 10550–10555 (2015).
(43) G.O. Guerrant and C.W. Moss, *Anal. Chem.* **56,** 633–638 (1984).
(44) G.Y. Qing, X.L. Li, P. Xiong, C. Chen, M.M. Zhan, X.M. Liang, and T.L. Sun, *ACS Appl. Mater. Inter.* **8,** 22084–22092 (2016).
(45) W.Y. Shao, J.X. Liu, K.G. Yang, Y. Liang, Y.J. Weng, S.W. Li, Z. Liang, L.H. Zhang, and Y.K. Zhang, *Talanta* **158,** 361–367 (2016).
(46) M.A. Lauber, Y.Q. Yu, D.W. Brousmiche, Z.M. Hua, S.M. Koza, P. Magnelli, E. Guthrie, C.H. Taron, and K.J. Fountain, *Anal. Chem.* **87,** 5401–5409 (2015).
(47) C.M. Woo, A.T. Iavarone, D.R. Spiciarich, K.K. Palaniappan, and C.R. Bertozzi, *Nature Methods* **12,** 561–567 (2015).
(48) J.A. Atwood, L. Cheng, G. Alvarez-Manilla, N.L. Warren, W.S. York, and R. Orlando, *J. Proteome Res.* **7,** 367–374 (2008).
(49) J.T. Cox, S.R. Kronewitter, A.K. Shukla, R.J. Moore, R.D. Smith, and K.Q. Tang, *Anal. Chem.* **86,** 9504–9511 (2014).
(50) H. Hinneburg, K. Stavenhagen, U. Schweiger-Hufnagel, S. Pengelley, W. Jabs, P.H. Seeberger, D.V. Silva, M. Wuhrer, and D. Kolarich, *J. Am. Soc. Mass Spectr.* **27,** 507–519 (2016).
(51) S.W. Wu, T.H. Pu, R. Viner, and K.H. Khoo, *Anal. Chem.* **86,** 5478–5486 (2014).
(52) B.J. Ko and J.S. Brodbelt, *Int. J. Mass Spectrom.* **377,** 385–392 (2015).
(53) C.J. Gray, B. Thomas, R. Upton, L.G. Migas, C.E. Eyers, P.E. Barran, and S.L. Flitsch, *BBA-Gen Subjects* **1860,** 1688–1709 (2016).
(54) D. Kolarich, E. Rapp, W.B. Struwe, S.M. Haslam, J. Zaia, R. Mcbride, S. Agravat, M.P. Campbell, M. Kato, R. Ranzinger, C. Kettner, and W.S. York, *Mol. Cell. Proteomics* **12,** 991–995 (2013).

Asif Shajahan and Parastoo Azadi are with the Complex Carbohydrate Research Center at the University of Georgia in Athens, Georgia. Direct correspondence to: azadi@ccrc.uga.edu ■

Applying LC with Low-Resolution MS/MS and Subsequent Library Search for Reliable Compound Identification in Systematic Toxicological Analysis

Systematic toxicological analysis (STA) is an important step in medicolegal investigations of death, poisoning, and drug use. The primary goal is the detection and confirmation of potentially toxic compounds in evidence. This article describes a workflow using nontargeted liquid chromatography–tandem mass spectrometry (LC–MS/MS) for reliable compound identification. Tandem mass spectrometry was performed on a low-resolution quadrupole-quadrupole-linear ion trap instrument. Acquired spectra were submitted to automated library search, and positive matches were verified by expert reviewing. After validation, the nontargeted LC–MS/MS technique was integrated in the STA service provided by our laboratory.

Florian Pitterl, Sebastian Köb, Johanna Pitterle, Julia Steger, and Herbert Oberacher

Systematic toxicological analysis (STA) is an important step in medicolegal investigations of death, poisoning, and drug use and can be done to various kinds of samples. The most frequently used biological samples are urine, blood, and plasma. In the field of post-mortem toxicology, additional specimens such as different tissues, gastric content, bile, and hair samples are analyzed. The samples are usually processed with generic extraction procedures, including liquid–liquid extraction and solid-phase extraction (SPE). As urine samples may contain phase II metabolites of drugs and poisons, a pretreatment step involving hydrolytic cleavage of the conjugate bond is commonly performed for this kind of sample.

Mass spectrometry (MS) hyphenated with a variety of separation techniques is the most important analytical technique applied to detect and confirm exogenous compounds present in biological samples. In particular, gas chromatography–mass spectrometry (GC–MS) is considered to be the gold standard for STA (1). This technique offers reliable identification of compounds because of the use of well-established mass spectral libraries. However, as one single mass spectrometric method is not able to cover the entire chemical space of forensic toxicological interest, GC–MS is usually complemented by liquid chromatography–mass spectrometry (LC–MS) techniques (2–7). Compound identification with LC–MS usually involves accurate molecular mass measurements (8–14), multiple reaction monitoring (MRM) (15–19), and acquisition of tandem mass spectra with subsequent library search (3–7, 20–37).

MRM is part of targeted assays. Such approaches provide very low limits of detection and quantitative information, but the number of compounds included is limited to a few hundred species only (21,23).

Nontargeted procedures usually use full-scan MS as the survey scan and combine it with data-dependent tandem mass spectrometry (MS/MS) scans (26). The automated switch from MS to MS/MS and back again is controlled by software. This data-dependent acquisition (DDA) enables recording of MS/MS spectra of almost all compounds detected in MS. An inherent limitation of DDA is the exclusion of low-abundant species particularly in complex samples because of the use of intensity thresholds and restriction of the number of ions submitted to fragmentation. To further increase detection sensitivity, data-independent acquisition (DIA) strategies were presented (29,34,35,37,38). In DIA, principally all ions detected in MS are submitted to MS/MS. One limitation of DIA is that this technique seems to work efficiently only on high-resolution instruments, such as quadrupole-quadrupole-time of flight (QqTOF), or orbital ion trap. Fourier transform ion cyclotron resonance (FT-ICR) instruments also belong to this class of instruments. They are, however, not common for this type of application. Furthermore, the full potential of DIA can only be exploited with data deconvolution algorithms that enable fast and efficient extraction of compound-specific tandem mass spectra. Irrespective of

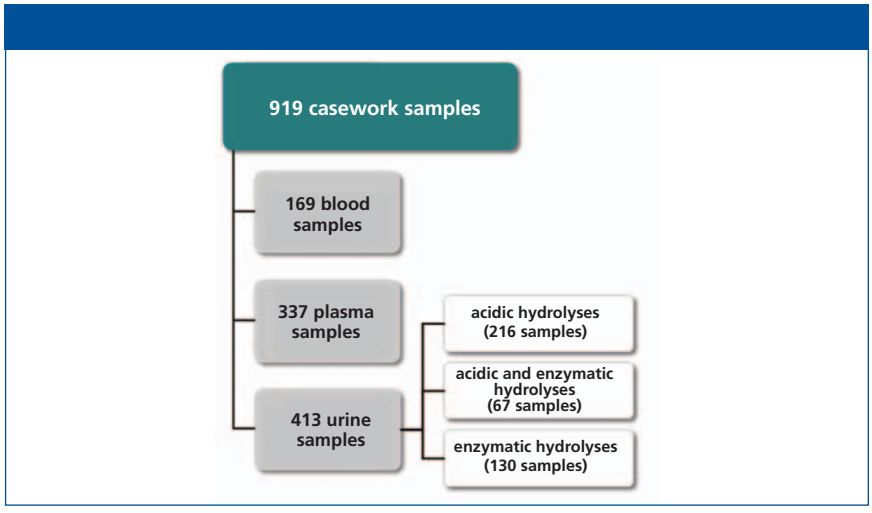

Figure 1: Types of authentic casework samples analyzed in this study.

the kind of acquisition control employed, by subsequent matching of the obtained MS/MS spectra to sufficiently large collections of high-quality reference spectra, such as MassBank (39), NIST (40), or the "Wiley Registry of Tandem Mass Spectral Data, MSforID" (41), unequivocal identification of thousands of compounds is feasible.

Initially, nontargeted LC–MS/MS methods with DDA were developed on low-resolution instruments (4,20,22,25,42). Currently, however, high-resolution QqTOF as well as orbital ion trap instruments are preferentially used for that purpose (8–10). The mass accuracy of these instruments is considered to represent a prime requisite for reliable compound identification. For instance, we have recently shown that a QqTOF instrument with DDA of MS/MS spectra and subsequent library search for STA of 65 authentic casework samples produced only 1.0% false positive results (3). In contrast, STA procedures involving automated library search with low-resolution data were reported to produce a significantly higher number of false positive results (31,43).

Wissenbach and colleagues tested the performance and transferability of their tandem mass spectral library (31). The group built a linear ion trap (LIT) library of MS^n spectra covering 4500 compounds. They analyzed 100 authentic urine samples with two LC–MS/MS-based screening strategies: (1) a LC–MS^n approach using a LIT instrument and (2) a LC–MS/MS approach using a quadrupole-quadrupole-linear ion trap (QqLIT) instrument. To improve performance of the library for QqLIT spectra, MS^n library spectra were merged. Automated library search was accomplished with "X-Rank" (44). The MS^n data produced 3362 positive matches; 1111 (33%) were found to be false positives by expert reviewing. The QqLIT data produced 3091 positive matches, and 1491 (48%) were found to be false positives.

Lynch and colleagues applied two different LC–MS/MS-based screening approaches for the analysis of 48 authentic urine samples (43). For both screening assays low-resolution instruments were used to generate MS/MS data. Identifications obtained by automated library search were checked by expert reviewing. The authors reported false positive rates of up to 37% and false negative rates of up to 49%. In the majority of cases, low quality spectra that were not efficiently handled by automated library search were identified as causes of incorrect matches.

Limited reliability of automated library search increases time and effort spent for expert reviewing of STA results. Accordingly, data processing is often regarded as a bottleneck. To overcome this limitation, advanced search algorithms showing increased tolerance against changes of fragment ion intensities are required. As such software tools have become available recently (44–47), the development of nontargeted LC–MS/MS methods with DDA and automated library search employing low-resolution instruments should be possible.

In this article, we present a nontargeted LC–MS/MS screening approach for STA of blood, plasma, and urine samples that uses low-resolution QqLIT for MS/MS spectra generation. The instrument is operated in positive electrospray ionization (ESI) mode with DDA. Sample processing involves a generic SPE method. Cleavage of the phase II metabolites in the urine samples is enabled by enzymatic hydrolysis. Chromatographic separations are accomplished with reversed-phase LC. The acquired MS/MS spectra were submitted to automated library search in the "Wiley Registry of Tandem Mass Spectral Data, MSforID." Putative correct positive matches are reviewed by an expert. The nontargeted LC–MS/MS method has been validated. Results of experiments assessing its selectivity, detection capabilities, and reliability of identification (sensitivity and specificity) are discussed. Finally, the usefulness of integrating the LC–MS/MS screening approach in our GC–MS-based analysis service will be demonstrated by giving an overview on the screening results obtained from 919 authentic samples submitted to STA from 2012 to 2014.

Materials and Methods

Chemicals and Samples

Water, methanol, sodium hydroxide, potassium hydroxide (all reagent grade), acetic acid (HOAc), heptafluorobutyric acid (HFBA), hydrochloric acid (37%), potassium dihydrogen phosphate (all puriss p.a.), ammonium hydroxide (25%), and ethyl acetate (all analytical reagent grade) were obtained from Sigma Aldrich. Phosphoric acid (86–87%, analytical reagent grade) was purchased from Scharlau. Propan-2-ol and dichloromethane (all analytical reagent grade) were supplied by Fisher Scientific. Acetic anhydride (extra pure) was obtained from Merck. Pyridine (AnalaR Normapur) was purchased from VWR. Bunitrolol hydrochloride was obtained from Chemicals International.

A 0.1 M phosphate buffer (pH 6.0) was prepared by adding appropriate amounts of potassium hydroxide to an aqueous solution of potassium dihydrogen phosphate.

Drug standards that were used for the preparation of spiked plasma samples were taken from the laboratory's collection. The standards were either obtained from commercial suppliers (Lipomed; LGC Promochem) or from the manufacturers of the marketed drugs.

For enzymatic hydrolysis of urine samples, a mixture of β-glucuronidase and

arylsulfatase (Helix pomatia, Roche Diagnostics) was used.

Blank urine samples were provided from healthy volunteers. Blank plasma samples were kindly donated by the blood bank of the Medical University of Innsbruck (Austria). The set of authentic casework samples consisted of 919 samples (blood, plasma, and urine) submitted to forensic toxicological examination (Figure 1). Sample collection was accomplished by medical doctors according to guidelines published by the "Österreichische Gesellschaft für Gerichtliche Medizin" (http://oeggm.com/oeggm-qualittssicherung.html). All samples were stored at -20 °C prior to analysis.

The STA Workflow

The setup of the developed STA workflow is shown in Figure 2. It involves sample preparation, data acquisition, and data mining steps.

Sample Preparation

Samples were processed with sample preparation workflows established in our laboratory for STA of blood, plasma, and urine (3).

Blood or plasma samples (2.0 mL) were mixed with 40 µL of an aqueous solution of the internal standard (IS, fencamfamine, 60 µg/mL) and diluted with 4 mL of distilled water as well as 4 mL of 0.1 M phosphate buffer (pH 6.0).

Acidic and/or enzymatic hydrolysis was used to cleave phase II metabolites in urine samples. For acidic hydrolysis, 10.0 mL of urine was split in two 5.0-mL aliquots. One aliquot was submitted to hydrolysis. Urine (5.0 mL) was mixed with 2.0 mL of 6 M hydrochloric acid. A 40 µL measure of an aqueous solution of fencamfamine (60 µg/mL) was added as internal standard. The sample was incubated in a microwave oven (450 W) for 60 s. After cooling, the samples were adjusted to pH 6 with sodium hydroxide and 4.0 mL of 0.1 M phosphate buffer (pH 6.0). The pH was checked with indicator paper. Finally, the hydrolyzed sample was mixed with the corresponding neat urine sample. For enzymatic hydrolysis, 10.0 mL of urine were mixed with 4.0 mL of 0.1 M phosphate buffer (pH 6.0), 40 µL of an aqueous solution of fencamfamine (60 µg/mL), and 200 µL of the enzyme solution (1.1 units β-glucuronidase and 0.52 units arylsulfatase, Roche Diagnostics). The sample was incubated for 16 h at 40 °C.

Prior to SPE, all preprocessed samples were centrifuged for 5 min at 4500*g*; only the supernatants were used. SPE was performed on Spe-ed Scan ABN columns (200 mg/3 mL, Applied Separations). Before application of the sample, the SPE column was conditioned with 2 mL methanol and 2 mL 0.1 M phosphate buffer (pH 6.0). Loading of sample was accomplished at a flow rate of 1.0–1.5 mL/min. Next, the column was washed with 3 mL of distilled water, 1 mL 1.0 M HOAc, and 1 mL of an aqueous methanol solution (5%, *v/v*), centrifuged for 5 min (4500*g*), and dried with a nitrogen stream. Elution was performed with 2.0 mL of a mixture of dichloromethane, propan-2-ol, and ammonium hydroxide (80/20/8, *v/v/v*). The eluate was split in two 1.0-mL aliquots. The aliquots were evaporated to dryness at 60 °C under a gentle stream of nitrogen. The residue of one aliquot was reconstituted in 50 µL of aqueous 0.5% HOAc/0.005% HFBA solution containing 5% methanol (*v/v*) and submitted to LC–MS/MS analysis. The residue of the second aliquot was reconstituted in 50 µL of ethyl acetate and submitted to GC–MS analysis. The GC–MS sample was analyzed in the native form and after derivatization. After evaporation to dryness at 60 °C under a gentle stream of nitrogen, 50 µL pyridine and 100 µL acetic anhydride were added. Derivatization was performed at 60 °C for 45 min. After evaporation of excess of derivatizing reagent, the residue was reconstituted in 50 µL ethyl acetate.

LC–MS/MS

The LC system consisted of a K-1001 pump (Knauer) and a HTS PAL autosampler (CTC Analytics) equipped with a 20-µL injection loop. The injected sample volume was 10 µL. Chromatographic separations were accomplished on a 100 × 2 mm, 5-µm, 100 Å Eurospher C18 column (Knauer) using a 10-min gradient of 5–100% methanol in aqueous 0.5% HOAc/0.005% HFBA solution. The column temperature was held at 50 °C with a column oven (Thermotechnic Products GmbH). The flow rate was set to 100 µL/min. The column outlet was directly connected to the ESI source.

ESI-MS was performed in the positive ion mode using a QqLIT instrument (3200 Q Trap, Sciex) equipped with a TurboIonSpray source (Sciex). Optimization of instrumental parameters was performed by infusion of 5.0 mg/L bunitrolol dissolved in aqueous 0.5% HOAc/0.005% HFBA solution containing 5% methanol (v/v) at a flow rate of 20 µL/min. The spray voltage was set to 5.5 kV. Gas flows of 45 arbitrary units for the nebulizer gas and 25 arbitrary units for the turbo gas were used. The temperature of the turbo gas was adjusted to 500 °C.

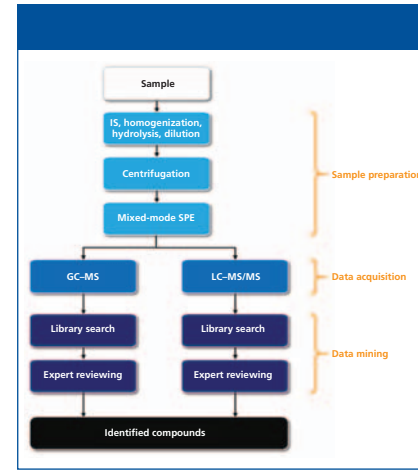

Figure 2: Workflow developed for STA with parallel GC–MS and LC–MS/MS analysis.

The mass spectrometer was operated under DDA control. A duty cycle in DDA mode included a Q3 MS scan followed by enhanced resolution (ER) scans and enhanced product ion (EPI) scans on the three most abundant precursor ions (processed in reverse order of abundance). The intensity threshold for triggering MS/MS experiments was 20,000 counts. Isolation of precursor ions was accomplished with Q1 set to unit resolution. The collision gas flow (N_2) was set to "high." For each precursor, MS/MS spectra were generated at a collision energy of 30 eV with a collision energy spread of 10 eV. Mass spectra were acquired from 135 to 700 *m/z*, and MS/MS spectra from 50 to 700 *m/z*. Accumulation times were set to 0.5 s for MS scans. The scan rate for ER scans and EPI scans was 1000 Da/s. Thus, the overall scan time per duty cycle was approximately 4.5 s. Spectra were recorded on a personal computer with Analyst software 1.5 (Sciex).

Library Search

Raw data files (.wiff) were converted to Mascot Generic Format (.mgf) files with the Sciex MS Data Converter (version 1.3

Table I: Evaluation of the detectability of 32 drugs in urine with LC–MS/MS under data-dependent acquisition control and subsequent library search.

Compound	Minimum Concentration that Enabled Identification by Library Search (ng/mL)
Cocaine	10
Ephedrine	10
Flunitrazepam	10
Hydroxyzine	10
Lidocaine	10
Methadone	10
Metoclopramide	10
Midazolam	10
Oxazepam	10
Atropine	25
Bisoprolol	25
Gliclazide	25
Ketamine	25
Metoprolol	25
Phenacetin	25
Tramadol	25
Venlafaxine	25
Alprazolam	50
Citalopram	50
Clobazam	50
Diclofenac	50
Diphenhydramine	50
Doxepine	50
Lamotrigine	50
Lorazepam	50
Mirtazapine	50
Prothipendyl	50
Ranitidine	50
Ethylmorphine	100
Quetiapine	100
Bromazepam	250
Olanzapine	250

beta). Next, the MS/MS spectra part of the .mgf file were extracted with a program written in ActivePerl 5.6.1 (Active State Corporation). Thus, all MS/MS spectra were available as plain text (ASCII) files containing peak list information, and they were used as input for library search.

The "Wiley Registry of Tandem Mass Spectral Data, MSforID" (Wiley) served as the reference library (41). The library was developed on a QqTOF instrument (Qstar XL, Sciex) using ESI in positive and negative ion mode. A detailed description of the instrumental parameters applied can be found elsewhere (47,48). At the current stage of development, the library contains 12,122 spectra of 1208 compounds.

The principles of the MSforID library search program have been described elsewhere (46,47,49). The search algorithm determines similarity between a sample spectrum and library spectra. The degree of similarity is expressed by two values: the "average match probability" (*mp*) and the "relative average match probability" (*ramp*), respectively. High compound-specific *amp*- and *ramp*-values indicate high similarity between the unknown and the reference compound. The substance with the highest amp- and ramp-values is considered to represent the unknown compound.

Automated MSforID search was performed with a program written in Pascal using Delphi 6 for Windows (Borland Software Corporation; now Embarcadero Technologies, Inc.) using the following search parameters: *m/z* tolerance of ±0.1, intensity cut-off factor of 0.01–0.05. The following criteria were used to classify obtained search results as putatively correct positive results: precursor ion mass tolerance of ±0.10, *amp* >10.0, and *ramp* >40.0. The accuracy of each putatively positive match was checked by expert reviewing.

GC–MS

The GC–MS system consisted of a HP7890 gas chromatograph with a HP5975C inert XL mass-selective detector (Agilent Technologies). A 30 m × 0.25 mm, 0.25-µm DB-XLB column (J&W Scientific) was used for chromatographic separation. Carrier gas was helium with a flow rate of 1.0 mL/min. Injection volume was 2 µL (splitless) and injection temperature was 250 °C. The temperature program was as follows: 50 °C, hold 1 min; increase to 150 °C with 25 °C/min, to 320 °C with 10 °C/min, hold for 8 min and to 330 °C in 20 °C/min, hold for 7.5 min. MS was performed in electron impact mode (70 eV) scanning from 50 to 600 *m/z*. Mass spectral data were recorded on a personal computer with the HP MS ChemStation software G1034C version D01.00 (Agilent Technologies) including the Maurer/Pfleger/Weber 2011 mass spectral library (Wiley) for compound identification.

Performance Evaluation

Evaluation of the performance of the nontargeted LC–MS/MS method developed for STA of urine, blood, and plasma samples was accomplished according to published recommendations for the validation of qualitative methods (50–52). The following performance parameters were examined: selectivity, detection capability, and reliability of identification (sensitivity and specificity).

Selectivity of the LC–MS/MS procedure and specificity of automated library search were evaluated by analyzing nine blank plasma samples and eight blank urine samples. All extracts were analyzed twice. The origin and plausibility of correct positive results was evaluated. Furthermore, the rate of false positive matches was determined to estimate specificity of the screening assay.

For evaluation of the detection capability of the LC–MS/MS method and the sensitivity of automated library search, spiked plasma and urine samples were analyzed. Blank plasma samples were fortified with 66 compounds at concentrations equal to the individual lower limits of the therapeutic blood/plasma ranges. A list of the compounds studied is provided in the Electronic Supplementary Material (ESM) Table S1 at: www.chromatographyonline.com/applying-lc-low-resolution-msms-and-subsequent-library-search-reliable-compound-identification-syste**.** Therapeutic ranges were extracted from the literature (53). Blank urine samples were spiked with 32 compounds at six different concentration levels (10 ng/mL, 25 ng/mL, 50 ng/mL, 100 ng/mL, 250 ng/mL, and 500 ng/mL). A list of the compounds studied can be found in Table I. The samples were analyzed, and the minimum concentrations enabling identification of the compounds by automated library search were determined.

A further proof of the reliability of the developed LC–MS/MS screening approach was obtained by analyzing 919 authentic casework samples (Figure 1). For benchmarking, GC–MS was used as a reference method. To simplify the comparison, multiple matches to a single reference compound were handled as one match only. Furthermore, all matches indicating intake of a certain drug compound (that is, the drug itself, metabolites as well as artifacts) were combined to one entry in the hit list (= "identified compound").

The following example may illustrate this modus operandi: if LC–MS/MS screening of a sample produces five MS/MS spectra that are matched to cocaine and several more spectra that are matched to benzoylecgonine and methylecgonine, then the five cocaine matches as well as the benzoylecgonine and methylecgonine matches are combined to the hit list entry "cocaine." Endogenous compounds (for example, adenine) as well as commonly observed nutritional compounds (caffeine and nicotine) were not included in the statistical evaluation of the results obtained.

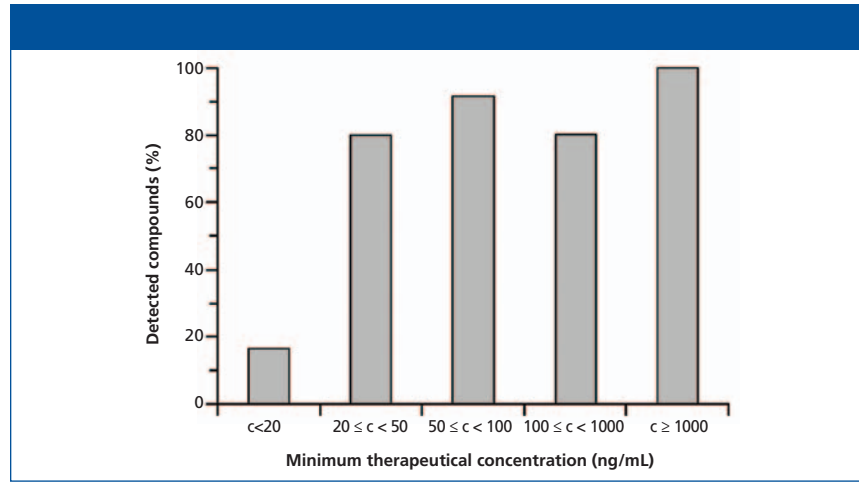

Figure 3: Impact of the plasma concentration on the detectability of 66 representative compounds with LC–MS/MS.

Results and Discussion

Evaluation of the Performance of the LC–MS/MS Method

Method validation is the process of sufficiently developing a picture of the performance of a method to demonstrate that it is fit for an intended purpose. To demonstrate the usefulness of the LC–MS/MS method for STA, the following parameters were studied: selectivity, detection capability, and reliability of identification (sensitivity and specificity).

Selectivity of the developed LC–MS/MS method and specificity of automated library search were tested by analyzing nine plasma and eight urine samples donated from volunteers who did not consume any drug. All extracts were screened twice by nontargeted LC–MS/MS.

The plasma samples produced 11,306 spectra; 136 spectra gave rise to correct positive identifications, nine matches were found to be incorrect. Thus, the false positive rate of automated library search was 0.08% only.

The urine samples produced 11,687 spectra; 237 spectra gave rise to correct positive identifications, 56 matches were found to be incorrect. Thus, the false positive rate of automated library search was 0.48% only.

The compounds correctly identified included the internal standard, nutritional compounds (caffeine, piperine), and endogenous compounds (adenine).

Automated library search was found to be very specific (>99%). The observed false positive rates were comparable to values previously reported for high-resolution instruments (2,35). As the low number of false positive matches produced by software were sorted out by expert reviewing, the LC–MS/MS procedure clearly passed the selectivity test.

Detection capabilities of the developed LC–MS/MS method and sensitivity of automated library search were tested by analyzing blank plasma and urine samples fortified with reference standards. For plasma, the lower end of the therapeutic range was defined as the minimum required performance limit at which a compound should be reliably detected and confirmed (3). To test detection sensitivity, blank plasma samples were spiked with 66 compounds present at concentrations equal to the individual lower limits of their therapeutic ranges and analyzed by LC–MS/MS. The obtained results are summarized in Figure 3. Down to a minimum therapeutic concentration of 20 ng/mL, the developed LC–MS/MS assay represents an efficient screening tool. More than 80% of all compounds were detected and identified. There were only four compounds with a minimum therapeutic concentration of ≥100 ng/mL that were not detected. For 3,4-methylenedioxymethamphetamine (MDMA) and 3,4-methylenedioxyamphetamine (MDA), in-source fragmentation might have negatively affected detectability. Fluoxetine produced an inconclusive fragmentation pattern at the collision energy settings employed, and diclofenac contained an acidic group that obviously had a negative effect on ionization efficiency.

In terms of the detection limits, the LC–MS/MS method was less efficient than our previously presented QqTOF method (3). Nevertheless, as with the detection sensitivity provided the majority of compounds were detectable and identifiable at therapeutic and thus even at the higher toxic and comatose-fatal blood-plasma concentrations (53), we regard the herein presented LC–MS/MS method sufficiently sensitive for application in STA.

To characterize the detection capabilities of the LC–MS/MS method for urine samples, limits of detection (LOD) values were determined for 32 compounds. Blank urine samples were spiked with test compounds at six different concentration levels (10 ng/mL, 25 ng/mL, 50 ng/mL, 100 ng/mL, 250 ng/mL, and 500 ng/mL). The samples were analyzed and the minimum concentrations enabling identification of the compounds by automated library search were determined (Table I). The majority of compounds were detectable at concentrations ≤50 ng/mL (87.5%). Ethylmorphine, quetiapine, bromazepam, and olanzapine showed higher LOD values.

The detection capabilities of the presented workflow are sufficient to enable application in STA. We believe, however, that more modern instrumentation will provide lower limits of detection, which would significantly improve detection capabilities of the nontargeted LC–MS/MS workflow described.

The tandem mass spectral data obtained from testing the detection capabilities of the LC–MS/MS method were further used to characterize sensitivity of automated library search. Sensitivity (also called the true positive rate or the recall rate) measures the proportion of actual positives, which are correctly identified as such. We defined a positive as a reference compound spiked in a sample that trig-

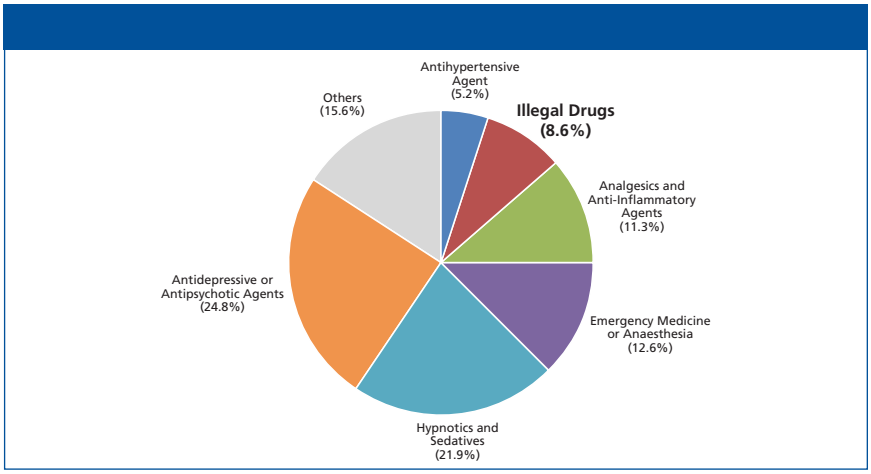

Figure 4: Important drug classes found in 169 plasma and 337 blood samples.

gered the acquisition of one or more MS/MS spectra in DDA mode. A true positive identification was obtained if one of the spectra representing a positive returned a classified match (precursor ion mass tolerance of ±0.10, *amp* >10.0, and *ramp* >40.0) to the corresponding reference compound from an automated library search. With both sets of spiked samples, 198 positives were generated, and only two of them produced false negative results (ethylmorphine at 50 ng/mL and bromazepam at 100 ng/mL in urine). Thus, sensitivity of automated library search was found to be 99%.

Application of the STA Workflow to the Analysis of Forensic Casework Samples

After demonstrating that the developed LC–MS/MS method is fit for purpose, we decided to integrate it into the GC–MS-based STA workflow part of the forensic-toxicological analysis service offered by our laboratory (Figure 2). This was realized in June 2012. By October 2014, 919 casework samples, including ante- and post-mortem samples, were analyzed with this parallel screening approach (Figure 1).

From June 2012 to October 2014, 169 blood samples and 337 plasma samples were received by the casework unit. STA of these samples led to 629 identifications. In 345 cases (54.8%), the presence of a compound was confirmed by LC–MS/MS and GC–MS, in 139 cases by LC–MS/MS only (22.0%), and in 145 cases by GC–MS only (23.0%). As expected, parallel screening with complementary mass spectrometric methods was a competent approach to increase reliability and validity of STA. In the majority of cases, identification was based on the results obtained by two independent methods. Furthermore, some compounds were preferentially detected by one of the two methods applied. LC–MS/MS was found to be particularly useful for the detection of beta blockers and benzodiazepines. Compounds with low-ionization efficiency in positive ESI (for example, propofol, diclofenac, ibuprofen, and barbiturates), on the other hand, were preferentially detected by GC–MS.

With 629 identifications obtained from the 506 blood or plasma samples, consumption of 124 different drug compounds was confirmed. An overview on important compound classes observed is provided in Figure 4. Out of the 629 identifications, 156 (24.8%) involved antidepressive or antipsychotic agents, such as citalopram, trazodone, quetiapine, mirtazapine, and prothipendyl. Other commonly observed medications belonged to the classes of hypnotics, sedatives, anesthetics, and analgesics. These kinds of drugs are commonly used in emergency medicine and critical care, and included midazolam, diazepam, lidocaine, propofol, and ketamine. Illegal drugs (morphine, methadone, cocaine, and MDMA) were identified in 8.6% of cases.

From June 2012 to October 2014, 413 urine samples were analyzed (Figure 1), and 1036 identifications were obtained. With this information, consumption of 165 different drug compounds was confirmed.

Processing of urine samples included a hydrolysis step to cleave phase II metabolites. In 2013, the hydrolysis protocol was changed from acidic hydrolysis to enzymatic hydrolysis with β-glucuronidase and arylsulfatase. To demonstrate the usefulness of this workflow modification, 67 urine samples were processed with both cleavage methods (Figure 1). Acidic hydrolysis enabled 153 identifications, and enzymatic treatment enabled 161 identifications. In particular, the detectability of benzodiazepines was found to be improved with the latter method.

Overall 197 urine samples were analyzed with the workflow that involved enzymatic hydrolysis (Figure 1) and 523 identifications were obtained. In 291 cases (55.6%), the presence of a compound was confirmed by LC–MS/MS and GC–MS, in 46 cases by LC–MS/MS only (15.8%), and in 186 cases by GC–MS only (28.6%).

With the 186 identifications obtained by GC–MS only, consumption of 64 different compounds was verified. There were three different reasons why LC–MS/MS was not able to detect or identify these species: (1) The compound was only included in the GC–MS library (31% of cases); (2) The compound was included in both libraries; identification was based on matches to transformation products or artifacts, which were only included in the GC–MS library (27% of cases); (3) The compound was included in both libraries; the compound was detected by GC–MS only (42% of cases).

Despite considerable success of the developed LC–MS/MS screening procedure, the limited number of compounds included in the tandem mass spectral library seems to be a shortcoming. With 1208 compounds, our library covers only part of the entire chemical space of potentially toxic compounds. Furthermore, some important drug metabolites and artifacts are missing. Both limitations are currently being addressed. We hope that these problems will be solved with a revised and extended version of the library.

A further shortcoming is the limited detection sensitivity of acidic compounds in positive ESI. This problem will be addressed by developing a nontargeted LC–MS/MS screening procedure with negative ESI.

Conclusions

STA is an integral part of the medicolegal investigation of death, poisoning, and drug use. The outcome of STA can have substantial legal and social consequences. Accordingly, the probability of a false result should be minimized by applying generic analyti-

cal techniques that enable sensitive detection and reliable identification of a large number of potentially toxic compounds. As a result of the complementarity of GC–MS and LC–MS/MS, we and others have shown that parallel screening with both methods is a competent STA strategy (2–7). With this study we provide further evidence for the usefulness of this approach.

The presented nontargeted LC–MS/MS method was developed on a low-resolution QqLIT instrument. Validation experiments clearly proved its fitness for STA of plasma, blood, and urine samples. The suitability of the developed LC–MS/MS screening approach for application in a forensic-toxicological analysis service was demonstrated by screening 919 casework samples, including ante- and post-mortem samples. STA led to >1600 identifications. More than 160 different drug compounds were detectable, and those included antidepressants, antipsychotics, hypnotics, sedatives, anaesthetics, analgesics, and illegal drugs.

It bears mentioning that our approach involved a QqLIT instrument for data acquisition and a tandem mass spectral library developed on a QqTOF instrument for identification. Nevertheless, sensitivity and specificity of an automated library search were found to be ≥99%. This observation clearly demonstrates that a database consisting of a properly designed tandem mass spectral library and a tailor-made search algorithm can be transferred between different types of instruments to enable reliable compound identification in authentic casework samples.

Despite considerable success of the developed STA procedure, there is still room for improvements. Problems related to detection sensitivity will be overcome by using more modern instrumentation and screening in negative ESI. Shortcomings of the tandem mass spectral library will be addressed by increasing its content. In particular, spectra of important drug metabolites and artifacts will be added.

Acknowledgments

We want to thank the members of our casework unit (Institute of Legal Medicine, Medical University of Innsbruck) for their assistance.

References

(1) H.H. Maurer, *J. Mass Spectrom.* **41,** 1399–1413 (2006).
(2) H. Oberacher and K. Arnhard, *Bioanalysis* **7,** 2825–2840 (2015).
(3) H. Oberacher, B. Schubert, K. Libiseller, and A. Schweissgut, *Anal. Chim. Acta* **770,** 121–131 (2013).
(4) F.L. Sauvage, F. Saint-Marcoux, B. Duretz, D. Deporte, G. Lachatre, and P. Marquet, *Clin. Chem.* **52,** 1735–1742 (2006).
(5) D.M. Mueller, B. Duretz, F.A. Espourteille, and K.M. Rentsch, Anal. *Bioanal. Chem.* **400,** 89–100 (2011).
(6) D.K. Wissenbach, M.R. Meyer, D. Remane, A.A. Philipp, A.A. Weber, and H.H. Maurer, *Anal. Bioanal. Chem.* **400,** 3481–3489 (2011).
(7) S. Broecker, S. Herre, B. Wüst, J. Zweigenbaum, and F. Pragst, *Anal. Bioanal. Chem.* **400,** 101–117 (2011).
(8) M.R. Meyer, A.G. Helfer, and H.H. Maurer, *Bioanalysis* **6,** 2275–2284 (2014).
(9) I. Ojanpera, M. Kolmonen, and A. Pelander, *Anal. Bioanal. Chem.* **403,** 1203–1220 (2012).
(10) A.H. Wu, R. Gerona, P. Armenian, D. French, M. Petrie, and K.L. Lynch, *Clin. Toxicol.* **50,** 733–742 (2012).
(11) M. Gergov, B. Boucher, I. Ojanpera, and E. Vuori, *Rapid Commun. Mass Spectrom.* **15,** 521–526 (2001).
(12) A. Pelander, I. Ojanpera, S. Laks, I. Rasanen, and E. Vuori, *Anal. Chem.* **75,** 5710–5718 (2003).
(13) A. Polettini, R. Gottardo, J.P. Pascali, and F. Tagliaro, *Anal. Chem.* **80,** 3050–3057 (2008).
(14) R.I.D. Birkler, R. Telving, O. Ingemann-Hansen, A.V. Charles, M. Johannsen, and M.F. Andreasen, *Forensic Sci. Int.* **222,** 154–161 (2012).
(15) D. Montenarh, M. Hopf, H.H. Maurer, P. Schmidt, and A.H. Ewald, *Anal. Bioanal. Chem.* **406,** 803–818 (2014).
(16) M. Di Rago, E. Saar, L.N. Rodda, S. Turfus, A. Kotsos, D. Gerostamoulos, and O.H. Drummer, *Forensic Sci. Int.* **243,** 35–43 (2014).
(17) D. Remane, D. Wetzel, and F.T. Peters, *Anal. Bioanal. Chem.* **406,** 4411–4424 (2014).
(18) M. Fisichella, L. Morini, C. Sempio, and A. Groppi, *Anal. Bioanal. Chem.* **406,** 3497–3506 (2014).
(19) S. Strano-Rossi, S. Odoardi, M. Fisichella, L. Anzillotti, R. Gottardo, and F. Tagliaro, *J. Chromatogr. A* **1372,** 145–156 (2014).
(20) F. Saint-Marcoux, G. Lachâtre, and P. Marquet, *J. Am. Soc. Mass Spectrom.* **14,** 14–22 (2003).
(21) C.A. Mueller, W. Weinmann, S. Dresen, A. Schreiber, and M. Gergov, *Rapid Commun. Mass Spectrom.* **19,** 1332–1338 (2005).
(22) S. Dresen, M. Gergov, L. Politi, C. Halter, and W. Weinmann, *Anal. Bioanal. Chem.* **395,** 2521–2526 (2009).
(23) S. Dresen, N. Ferreirós, H. Gnann, R. Zimmermann, and W. Weinmann, *Anal. Bioanal. Chem.* **396,** 2425–2434 (2010).
(24) F.L. Sauvage, N. Picard, F. Saint-Marcoux, J.M. Gaulier, G. Lachatre, and P. Marquet, *J. Sep. Sci.* **32,** 3074–3083 (2009).
(25) F.L. Sauvage and P. Marquet, *Anal. Bioanal. Chem.* **396,** 1947 (2010).
(26) T.N. Decaestecker, K.M. Clauwaert, J.F. Van Bocxlaer, W.E. Lambert, E.G. Van den Eeckhout, C.H. Van Peteghem, and A.P. De Leenheer, *Rapid Commun. Mass Spectrom.* **14,** 1787–1792 (2000).
(27) T.N. Decaestecker, S.R. Vande Casteele, P.E. Wallemacq, C.H. Van Peteghem, D.L. Defore, and J.F. Van Bocxlaer, *Anal. Chem.* **76,** 6365–6373 (2004).
(28) H.C. Liu, R.H. Liu, H.O. Ho, and D.L. Lin, *Anal. Chem.* **81,** 9002–9011 (2009).
(29) H.K. Lee, C.S. Ho, Y.P. Iu, P.S. Lai, C.C. Shek, Y.C. Lo, H.B. Klinke, and M. Wood, *Anal. Chim. Acta* **649,** 80–90 (2009).
(30) D.K. Wissenbach, M.R. Meyer, D. Remane, A.A. Weber, and H.H. Maurer, *Anal. Bioanal. Chem.* **400,** 79–88 (2011).
(31) D.K. Wissenbach, M.R. Meyer, A.A. Weber, D. Remane, A.H. Ewald, F.T. Peters, and H.H. Maurer, *J. Mass Spectrom.* **47,** 66–71 (2012).
(32) S. Broecker, S. Herre, and F. Pragst, *Forensic Sci. Int.* **218,** 68–81 (2012).
(33) H.R. Lin, C.C. Liao, and T.C. Lin, *Rapid Commun. Mass Spectrom.* **28,** 2043–2053 (2014).
(34) A.T. Roemmelt, A.E. Steuer, M. Poetzsch, and T. Kraemer, *Anal. Chem.* **86,** 11742–11749 (2014).
(35) K. Arnhard, A. Gottschall, F. Pitterl, and H. Oberacher, *Anal. Bioanal. Chem.* **407,** 405–414 (2015).
(36) J. Kempf, J. Traber, V. Auwarter, and L.M. Huppertz, *Forensic Sci. Int.* **243,** 84–89 (2014).
(37) N.S. Chindarkar, M.R. Wakefield, J.A. Stone, and R.L. Fitzgerald, *Clin. Chem.* **60,** 1115–1125 (2014).
(38) J.D. Chapman, D.R. Goodlett, and C.D. Masselon, *Mass Spectrom. Rev.* **33,**

452–470 (2014).
(39) H. Horai, M. Arita, S. Kanaya, Y. Nihei, T. Ikeda, K. Suwa, Y. Ojima, K. Tanaka, S. Tanaka, K. Aoshima, Y. Oda, Y. Kakazu, M. Kusano, T. Tohge, F. Matsuda, Y. Sawada, M.Y. Hirai, H. Nakanishi, K. Ikeda, N. Akimoto, T. Maoka, H. Takahashi, T. Ara, N. Sakurai, H. Suzuki, D. Shibata, S. Neumann, T. Iida, K. Tanaka, K. Funatsu, F. Matsuura, T. Soga, R. Taguchi, K. Saito, and T. Nishioka, *J. Mass Spectrom.* **45,** 703–714 (2010).
(40) X.Y. Yang, P. Neta, and S.E. Stein, *Anal. Chem.* **86,** 6393–6400 (2014).
(41) H. Oberacher, *The Wiley Registry of Tandem Mass Spectral Data, MSforID,* 1st Ed. (John Wiley & Sons, Hoboken, New Jersey, 2011).
(42) R.L. Fitzgerald, J.D. Rivera, and D.A. Herold, *Clin. Chem.* **45,** 1224–1234 (1999).
(43) K.L. Lynch, A.R. Breaud, H. Vandenberghe, A.H.B. Wu, and W. Clarke, *Clin. Chim. Acta* **411,** 1474–1481 (2010).
(44) R. Mylonas, Y. Mauron, A. Masselot, P.A. Binz, N. Budin, M. Fathi, V. Viette, D.F. Hochstrasser, and F. Lisacek, *Anal. Chem.* **81,** 7604–7610 (2009).
(45) H. Oberacher, G. Whitley, B. Berger, and W. Weinmann, *J. Mass Spectrom.* **48,** 497–504 (2013).
(46) H. Oberacher, M. Pavlic, K. Libiseller, B. Schubert, M. Sulyok, R. Schuhmacher, E. Csaszar, and H.C. Kofeler, *J. Mass Spectrom.* **44,** 494–502 (2009).
(47) M. Pavlic, K. Libiseller, and H. Oberacher, *Anal. Bioanal. Chem.* **386,** 69–82 (2006).
(48) M. Pavlic, B. Schubert, K. Libiseller, and H. Oberacher, *Forensic Sci. Int.* **197,** 40–47 (2010).
(49) H. Oberacher, M. Pavlic, K. Libiseller, B. Schubert, M. Sulyok, R. Schuhmacher, E. Csaszar, and H.C. Kofeler, *J. Mass Spectrom.* **44,** 485–493 (2009).
(50) C. Jimenez, R. Ventura, and J. Segura, *J. Chromatogr. B* **767,** 341–351 (2002).
(51) E. Trullols, I. Ruisanchez, and F.X. Rius, *Trends Anal. Chem.* **23,** 137–145 (2004).
(52) S. Cardenas and M. Valcarcel, *Trends Anal. Chem.* **24,** 477–487 (2005).
(53) M. Schulz and A. Schmoldt, *Pharmazie* **58,** 447–474 (2003).

Florian Pitterl is an analytical chemist who received his PhD at the University of Innsbruck, Austria, in 2010. After spending a year as postdoctoral fellow at the National Hellenic Research Foundation in Athens, Greece, he got a postdoc position at the Institute of Legal Medicine of the Medical University of Innsbruck. Since 2014 he has been lab head of the Forensic Toxicology Laboratory at the Institute of Legal Medicine. **Sebastian Köb, Johanna Pitterle, and Julia Steger** were masters students in the group of Herbert Oberacher. **Herbert Oberacher** is an analytical chemist who received his PhD at the University of Innsbruck, Austria, in 2002. After spending a year as a postdoctoral fellow at the University of the Saarland, Germany, he got a position as senior researcher at the Institute of Legal Medicine of the Innsbruck Medical University, Austria. In 2007 he received the "venia docendi" for bioanalysis, and in 2011 he was appointed to Associate Professor. His research focuses on the development of chromatographic, mass spectrometric, and bioinformatic techniques for the analysis of bioorganic molecules with special emphasis on small molecules and nucleic acids. He has (co-) authored more than 90 papers in international scientific journals and received several national and international awards. ■

AD INDEX

PRODUCTS & RESOURCES

HPLC system

The 1260 Infinity II Prime LC system from Agilent is designed to provide an extended pressure range (up to 800 bar), quaternary mixing, and specifically designed columns. According to the company, automated instrument features reduce the need for manual interaction, and the system's Intelligent System Emulation Technology (ISET) allows for method transfers from many Agilent and third-party legacy instruments.
Agilent Technologies,
Santa Clara, CA.
www.agilent.com

Solid-phase extraction plates

EVOLUTE HYDRO solid-phase extraction (SPE) plates from Biotage are designed with EVOLUTE SPE sorbents and Hydro frit technology. According to the company, the plates enable in situ in-well hydrolysis of urine samples, and sample cleanup is performed in the same plate, without the need to transfer samples.
Biotage,
Charlotte, NC.
www.biotage.com

Thermal desorber

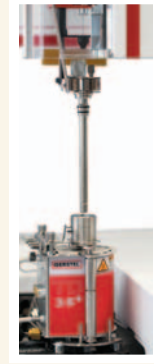

Gerstel's TD 3.5+ thermal desorber is designed for the analysis of material emissions, flavors, and air. According to the company, the thermal desorber operates with standard 3.5-in. tubes and Gerstel plus tubes with 30% more sorbent, and its liner-in-liner design reduces analyte loss and memory effects.
Gerstel GmbH & Co., KG,
Linthicum, MD.
www.gerstel.com

Gas generator

The Mistral EVO self-contained gas generator from VICI is designed to produce greater than 99% pure LC–MS-grade nitrogen gas with pressures up to 116 psig, and with flows up to 40 L/min. According to the company, all gases are produced using a combination of compressors, filtration, and high-performance pressure swing technologies.
VICI DBS Gas Generators,
Salem, NH.
Houston, TX. www.vicidbs.com

HILIC metabolomics brochure

A 2017 brochure of zwitterionic LC–MS columns for metabolomics applications is available from The Nest Group. According to the company, applications are shown for nucleotides, phospholipids, amino acids, cell metabolites, and artificial sweeteners, and scientific literature references are included that provide an objective overview of capabilities for silica and polymer-based, zwitterionic HILIC chemistries manufactured by HILICON AB.
The Nest Group, Inc., Southborough, MA.
www.nestgrp.com

EtG and EtS column

The Raptor ethyl glucuronide (EtG) and ethyl sulfate (EtS) column from Restek is designed to retain and resolve EtG and EtS from matrix interferences. According to the company, the column is suitable for alcohol consumption monitoring by high-throughput laboratories.
Restek Corporation,
Bellefonte, PA.
www.restek.com/raptor

Antibody bioanalysis kit

The nSMOL (nano-surface and molecular orientation limited proteolysis) antibody bioanalysis kit from Shimadzu is designed for the analysis of a variety of pharmaceutical antibodies. According to the company, the kit enables selective proteolysis of the Fab region of monoclonal antibodies to improve the productivity and robustness of LC–MS monoclonal antibody bioanalysis.
Shimadzu Scientific Instruments,
Columbia, MD.
www.ssi.shimadzu.com

Antibody analysis application note

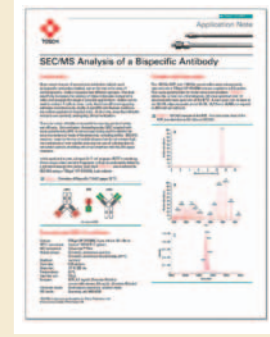

An application note titled "SEC/MS Analysis of a Bispecific Antibody" is available from Tosoh Bioscience. The publication describes how the accurate mass determination of a bispecific T-cell engager (BiTE) was analyzed by SEC–MS using a TSKgel 2-µm SEC column under non-denaturing conditions. According to the application note, no signs of particle shedding or sample carryover, which may interfere with MS signal response, were noted in the analysis. **Tosoh Bioscience, LLC,** King of Prussia, PA.
www.tosohbioscience.com

TOSOH BIOSCIENCE

Analysis of a Bispecific Antibody Using SEC–MS

Tosoh Bioscience

More potent formats of monoclonal antibodies (mAbs), such as bispecific antibodies (bsAbs), are on the rise in the area of biotherapeutics. Characterization of bsAbs is essential to ensuring product safety and efficacy. Size-exclusion chromatography (SEC) coupled with mass spectrometry (MS) is increasingly being used to identify the accurate molecular mass of biomolecules, including bsAbs. SEC–MS, however, requires the use of mobile phases that do not contain high concentrations of nonvolatile salts and the use of columns that do not exhibit particle shedding, both of which will interfere with the MS signal response.

In this application note, a bispecific T cell engager (BiTE®) consisting of two single-chain variable fragments (scFvs) recombinantly linked by a nonimmunogenic five-amino-acid chain was analyzed by SEC–MS using a TSKgel® UP-SW3000, 2 µm column.

Experimental HPLC Conditions

Column:	TSKgel UP-SW3000, 2 µm, 4.6 mm ID × 30 cm
HPLC Instrument:	Nexera® XR UHPLC system
MS Instrument:	Q Exactive™ Plus
Mobile phase:	20 mmol/L ammonium acetate, 10 mmol/L ammonium bicarbonate; pH 7.2
Flow rate:	0.35 mL/min
Detection:	UV @ 280 nm
Temperature:	30 °C
Injection vol.:	5.0 µL
Samples:	BiTE, 0.3 mg/mL (Creative Biolabs)
Ionization mode:	Electrospray ionization, positive mode
MS mode:	Scanning, *m/z* 800–6000

Results and Discussion

The ~55 kDa BiTE and parent mAbs (data not shown) were subsequently injected onto a TSKgel UP-SW3000 column coupled to a mass spectrometer for molar mass determination. Figure 1 shows the (a) total ion chromatogram, (b) mass spectrum, and (c) deconvoluted mass spectrum of the BiTE. A main peak can be seen at *m/z* 54,143; adjacent peaks at *m/z* 54,181, 54,219, and 54,086 correspond to different salt adducts.

Prior to analysis, a blank injection was run in order to assess column particle shedding. Figure 2a shows the total ion chromatogram of a blank injection. MS data indicates that there is no shedding from the TSKgel UP-SW3000 column prior to sample injection. Additionally, a blank injection was run between each of the sample injections in order to monitor sample carryover. Figure 2b shows the total ion chromatogram of a blank injection run between the BiTE and parent mAb showing no evidence of carryover.

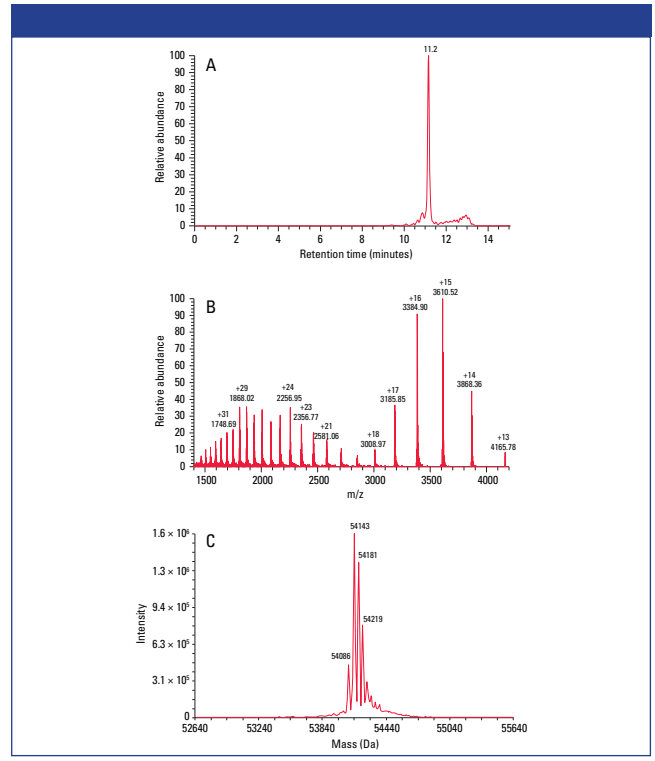

Figure 1: SEC–MS analysis of the BiTE. Accurate molar mass of the BiTE was identified as 54.1 kDa via SEC–MS.

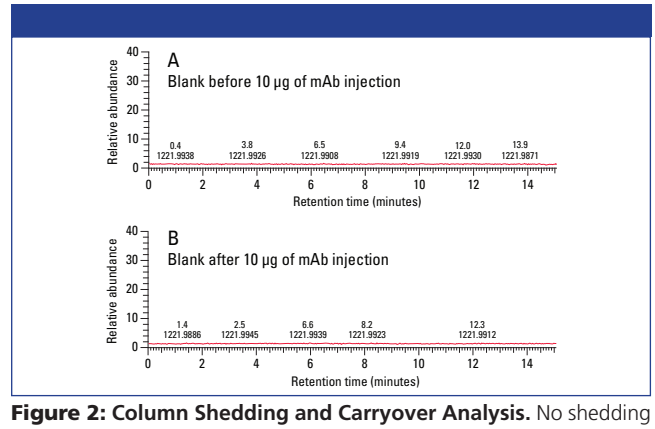

Figure 2: Column Shedding and Carryover Analysis. No shedding or carryover was observed via MS total ion chromatogram.

Conclusion

The TSKgel UP-SW3000, 2 µm SEC column can be used as a platform method for bispecific antibody accurate mass determination using SEC–MS. An MS-compatible mobile phase under nondenaturing condition was successfully used with the TSKgel UP-SW3000 column. No signs of particle shedding or sample carryover, which may interfere with MS signal response, were noted with the TSKgel UP-SW3000 column.

*SEC–MS analysis was performed by the Wistar Proteomics and Metabolomics Facility (Philadelphia, PA).

Tosoh Bioscience LLC
3604 Horizon Drive, Suite 100, King of Prussia, PA 19406
tel. (484) 805-1219, fax (610) 272-3028
Website: www.tosohbioscience.com

Validation of Horizon Technology Disk Extraction Technology for US EPA Wastewater Method 625.1

Zoe Grosser*, Alicia Cannon*, Michael Ebitson*, Melissa Lever*, Nic Rasnake†, Jessica Bowker†, Allen Fuller†, Chris Johnson†, *Horizon Technology, and †ESC Lab Sciences

The US EPA monitors a variety of chemicals in water that may cause harm to humans or wildlife to minimize exposure. Method 625 was developed by the Office of Science and Technology in the Clean Water program to allow the monitoring of a large suite of semivolatile chemicals in wastewater for compliance with the National Pollution Discharge Elimination System (NPDES). NPDES is a system of permitting that defines the characteristics of water that is released into a waterway, defined by industrial category. The permitting levels are set depending on the waterway's use. If the waterway is used for recreation or is an important wildlife habitat, the limit may be set lower.

The original method was developed in the early 1980s and has been updated several times since then to allow the use of more modern technology. The latest update has taken place over the last few years and was proposed in a Method Update Rule (MUR) in 2015 which was just published in the Federal Register August 28, 2017 and became effective September 27, 2017 (1). The latest version of the method includes a larger suite of analytes (up to 364) and an extensive set of labeled surrogates to better monitor the method performance throughout the sample preparation and analysis step.

Table I: Centralized waste treatment point source (437) matrix spike and spike duplicate results

Compound	Recovery (%)	Range P,Ps(%)	Pass/ Fail	RPD (%)	RPD (%) Limit	Pass/ Fail
Fluorene	99.6	59-121	Pass	6.89	38	Pass
Hexachlorobenzene	110	D-152	Pass	9.10	55	Pass
Hexachloro-1,3-butadiene	99.6	24-120	Pass	4.09	62	Pass
Hexachloroethane	61.6	40-120	Pass	16.1	52	Pass
Indeno(1,2,3-cd)pyrene	73.5	D-171	Pass	4.54	99	Pass
Isophorone	100	21-196	Pass	2.71	93	Pass
Naphthalene	96.0	21-133	Pass	2.49	65	Pass
Nitrobenzene	94.2	35-180	Pass	0.79	62	Pass
N-Nitrosodi-n-propylamine	113	D-230	Pass	2.55	87	Pass
Phenanthrene	97.2	54-120	Pass	7.33	128	Pass
Pyrene	90.9	52-120	Pass	8.40	49	Pass
1,2,4-Trichlorobenzene	90.2	44-142	Pass	5.68	50	Pass

This application note will present the data collected as part of the demonstration of disk solid phase extraction validation for US EPA method 625.1. Nine different wastewater matrices were evaluated and tested against the criteria listed in Table 6 of the method. Sample preparation was performed using the Atlantic® One-pass system, where the water sample is passed through a solid phase extraction (SPE) disk and carbon cartridge once, rather than twice with a pH change between loadings. Automation of the process was achieved using the SPE-DEX® 4790 system (superseded by SPE-DEX 5000). Table I shows the matrix spike and matrix spike duplicate results for a centralized waste treatment point source (437 NPDES category) sample, for selected compounds. The spike recovery and agreement between the duplicates was within criteria for most all analytes. Method detection limits, initial demonstration of compliance, and other wastewater matrices are shown in the full application note (2).

References

(1) Method 625.1, December 14 revision, can be found in the MUR, February 19, 2015. Or downloaded here: https://nepis.epa.gov/Exe/ZyPDF.cgi/P100LVHC.PDF?Dockey=P100LVHC.PDF

(2) Application Note 117, "Validation of Horizon Technology Disk Extraction Technology for US EPA Wastewater Method 625.1," available from www.horizontechinc.com.

Horizon Technology, Inc.
16 Northwestern Drive, Salem, NJ 03079
tel. (603) 893-3663
Website: www.horizontechinc.com

Rapid Perfluorinated Alkyl Acid Analysis by LC–MS/MS Increases Sample Throughput

Restek Corporation

- ***Raptor C18 SPP 5 µm core-shell silica particle columns offer excellent resolution for fluorochemicals with short total cycle times. For even faster analysis, 2.7 µm core-shell particles are available.***
- ***Meets EPA Method 537 requirements.***
- ***Unique, robust Raptor C18 column design increases instrument uptime.***

Perfluorinated alkyl acids are man-made fluorochemicals used as surface-active agents in the manufacture of a variety of products, such as firefighting foams, coating additives, textiles, and cleaning products. They have been detected in the environment globally and are used in very large quantities around the world. These fluorochemicals are extremely persistent and resistant to typical environmental degradation processes. As a result, they are widely distributed across the higher trophic levels and are found in soil, air, groundwater, municipal refuse, and landfill leachates. The toxicity, mobility, and bioaccumulation potential of perfluorooctanesulfonic acid (PFOS) and perfluorooctanoic acid (PFOA), in particular, pose potential adverse effects for the environment and human health.

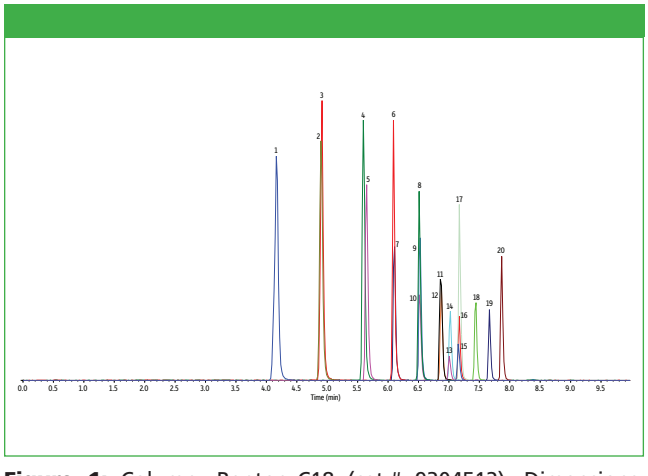

Figure 1: Column: Raptor C18 (cat.# 9304512); Dimensions: 100 mm × 2.1 mm ID; Particle size: 5 µm; Pore size: 90 Å; Temp.: 40 °C; Sample: Diluent: Methanol–water (96:4); Conc.: 5–10 ng/mL; Inj. vol.: 5 µL; Mobile phase: A: 5 mM ammonium acetate in water; B: Methanol; Gradient (%B): 0.00 min (10%), 8.00 min (95%), 8.01 min (10%), 10.0 min (10%); Flow: 0.4 mL/min; Detector: MS/MS; Ion source: Electrospray; Ion mode: ESI-; Mode: MRM.

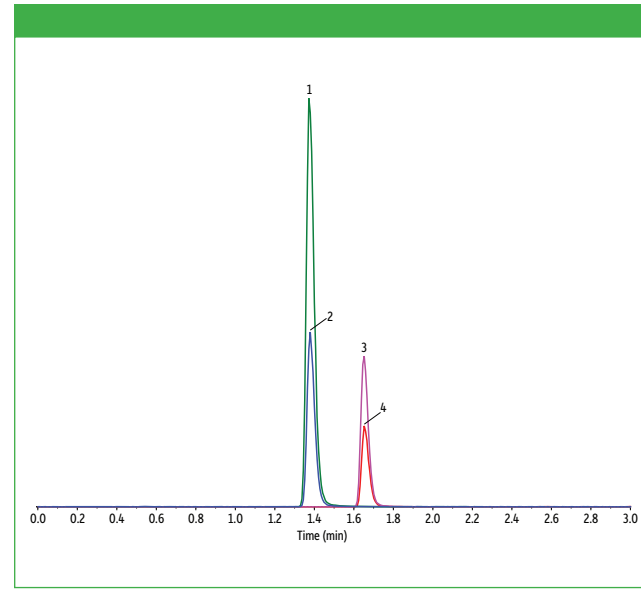

Figure 2: Column: Raptor C18 (cat.# 9304512); Dimensions: 100 mm × 2.1 mm ID; Particle size: 5 µm; Pore size: 90 Å; Temp.: 40 °C; Sample: Diluent: Water–methanol (50:50); Conc.: 5–10 ng/mL; Inj. vol.: 5 µL; Mobile phase: A: 5 mM ammonium acetate in water; B: Methanol; Gradient (%B): 0.00 min (60%), 2.50 min (95%), 2.51 min (60%), 4.50 min (60%); Flow: 0.4 mL/min; Detector: MS/MS; Ion mode: ESI-; Mode: MRM; Instrument: UHPLC.

Perfluorinated alkyl acid analysis can be challenging because these compounds are chemically different from most other environmental contaminants. They are difficult to quantify because some are more volatile than others, and they also tend to be more hydrophilic and somewhat reactive. In addition, fluorochemicals are present in polytetrafluoroethylene (PTFE) materials, so excluding the use of any PTFE labware throughout the sampling and analytical processes (including HPLC solvent inlet tubing) is essential for accurate analysis. Typically, perfluorinated alkyl acids are analyzed by LC–MS/MS methods, such as EPA Method 537, but long analysis times can significantly limit sample throughput.

As written, the EPA 537 requires a 27-min cycle per sample, but the method does allow flexibility in the column used as long as there is sufficient resolution for the MS dwell time for all compounds in a specific retention time window. In Figure 1, all target perfluorinated alkyl acids were analyzed

Table I: Peak identifications for Figure 1

Peaks	t_R (min)	Conc. (ng/mL)	Precursor Ion	Product Ion
1. Perfluorobutanesulfonic acid (PFBS)	4.17	5	298.9	79.9
2. Perfluoro-*n*-[1,2-$^{13}C_2$]hexanoic acid (^{13}C-PFHxA)	4.90	5	314.8	269.8
3. Perfluorohexanoic acid (PFHxA)	4.91	5	312.7	268.9
4. Perfluoroheptanoic acid (PFHpA)	5.59	5	362.8	318.8
5. Perfluorohexanesulfonic acid (PFHxS)	5.65	5	398.8	79.8
6. Perfluoro-[1,2-$^{13}C_2$]octanoic acid (^{13}C-PFOA)	6.09	5	414.8	369.8
7. Perfluorooctanoic acid (PFOA)	6.10	5	412.7	368.8
8. Perfluoro-1-[1,2,3,4-$^{13}C_4$]octanesulfonic acid (^{13}C-PFOS)	6.51	10	502.7	79.9
9. Perfluorooctanesulfonic acid (PFOS)	6.52	5	498.7	79.9
10. Perfluorononanoic acid (PFNA)	6.52	5	462.6	418.9
11. Perfluoro-*n*-[1,2-$^{13}C_2$]decanoic acid (^{13}C-PFDA)	6.87	5	514.8	469.9
12. Perfluorodecanoic acid (PFDA)	6.88	5	512.7	468.8
13. N-deuteriomethylperfluoro-1-octanesulfonamidoacetic acid (d3-NMeFOSAA)	7.01	10	572.7	418.9
14. N-methyl perfluorooctanesulfonamidoacetic acid (NMeFOSAA)	7.02	10	569.8	418.9
15. N-deuterioethylperfluoro-1-octanesulfonamidoacetic acid (d5-NEtFOSAA)	7.16	10	588.8	418.9
16. N-ethyl perfluorooctanesulfonamidoacetic acid (NEtFOSAA)	7.17	10	583.8	418.9
17. Perfluoroundecanoic acid (PFUnA)	7.17	10	562.8	518.8
18. Perfluorododecanoic acid (PFDoA)	7.44	10	612.7	568.8
19. Perfluorotridecanoic acid (PFTrDA)	7.67	10	662.7	618.8
20. Perfluorotetradecanoic acid (PFTA)	7.87	10	712.8	668.9

Column description

Raptor C18 LC Columns (USP L1)

Description	cat.#
5 µm Columns	
100 mm, 2.1 mm ID	9304512

on a Raptor C18 column in under 8 min with a total cycle time of 10 min—resulting in an approximately three-fold faster analysis than the EPA method. While this analysis is significantly faster, there is no sacrifice in peak resolution or selectivity, meaning all fluorochemicals are easily identified and they elute as highly symmetrical peaks that can be accurately integrated and quantified by MS/MS. If PFOA and PFOS are the only target fluorochemicals, the analysis can be further optimized, which results in a fast, <2-min separation with a total cycle time of just 4.5 min, as shown in Figure 2.

Whether labs conducting perfluorinated alkyl acid analysis by LC use longer target analyte lists or focus just on PFOA and PFOS, the excellent peak shapes and separations achieved here result in consistent, accurate quantification with much shorter analysis times. By switching to a Raptor C18 column, labs can process more samples per hour while still meeting fluorochemical method requirements.

Restek Corporation
110 Benner Circle, Bellefonte, PA 16823
tel. (800) 356-1688, fax (814) 353-1309
Website: www.restek.com

Enlist the Power of Automation

GERSTEL provides customer focused solutions for GC/MS and LC/MS adapted to your requirements. Add the power of automation and solvent free, or solvent reduced, analyte concentration techniques to your sample preparation:

- Liquid/Liquid Extraction
- Clean-Up: SPE and Filtration
- Generating and Adding standards
- Mixing, Centrifugation and Evaporation
- (Dynamic) Headspace, Large or Small…

GERSTEL Solutions enhance performance and throughput, produce excellent results and are easily adapted to new tasks.

What can we do for you?

Derivatization, Adding Standards

SPE, Online SPE (SPE^{XOS})

Filtration, Clean Up

SPME, SBSE, Thermal desorption

Headspace & Dynamic Headspace (DHS)

Sample Prep by mouse-click (MAESTRO)

Agilent Technologies
Premier Solution Partner

GERSTEL

GERSTEL 50

www.gerstel.com